

# INFLUENCE OF PEKAR ADDITIONAL LIGHT WAVES ON OPTICAL SPECTRA OF CRYSTALS (REVIEW)

M.I. STRASHNIKOVA

UDC 535.343.2;535.548

©2007

Institute of Physics, Nat. Acad. Sci. of Ukraine

(46, Nauky Ave., Kyiv 03680, Ukraine; e-mail: strashnik@iop.kiev.ua)

*To the 90-th anniversary of the birthday of S.I. Pekar*

Experimental works, which confirm the existence of additional light waves (ALWs) in the exciton resonance range predicted by S.I. Pekar in 1957, have been reviewed. The scope of the review includes works concerning the measurements of absorption, reflection, and scattering spectra and the spectra of phase changes of a reflected light wave, as well as the measurements of the refractive index dispersion. The works concerning the spatial separation of Pekar waves in thin wedge-shaped crystals have been considered in detail. A transition to classical single-wave crystal optics, which takes place after achieving some critical value of the exciton damping constant, has been traced. The applicability criteria of classical Kramers–Kronig relations (KKRs) and Fresnel formulas for the determination of optical characteristics of crystals have been presented. The characteristic features of the approximation of reflection spectra under different additional boundary conditions (ABCs) have been analyzed, as well as the influence of surface treatment on the profiles of exciton reflection spectra.

## CONTENTS

### 1. Introduction

### 2. Fundamentals of Pekar's Theory and Single-wave Optics

#### 2.1. Spatial dispersion. Pekar's theory

#### 2.2. Classical crystal optics

### 3. Manifestations of an Additional Wave at Frequencies above $\omega_L$

#### 3.1. Interference spectra of thin crystals

#### 3.2. Mandelshtam–Brillouin resonance scattering

#### 3.3. Direct measurements of the group velocity of light waves

#### 3.4. Light refraction by a wedge-shaped crystal

### 4. Manifestations of an Additional Wave below the Frequency $\omega_L$

#### 4.1. Violation of KKR's

##### 4.1.1. Comparison of the dependences calculated by KKR's and measured experimentally

#### 4.2. Invalidity of Fresnel formulas

##### 4.2.1. Spectral dependence of the reflection coefficient

##### 4.2.2. Spectral dependence of the reflected wave phase variation

#### 4.3. Dependence of the refractive index on the crystal thickness

### 5. Temperature Dependence of Spatial Dispersion Effects and Transition to Classical Crystal Optics

#### 5.1. Absorption

#### 5.2. Dispersion of the refractive index

### 6. Influence of the Surface on the Reflection Spectra of Crystals and the Features of Their Approximation

#### 6.1. ABCs and theoretical models of surface influence

#### 6.2. Comparison with experiment

### 7. Applicability Scope of KKR's in the Presence of ALW

#### 7.1. Dispersion and absorption curves

#### 7.2. Application of KKR's to reflection spectra

### 8. Topicality of ALW Researches

### 9. Modern Trends in Studying ALWs

### 10. Conclusions

## 1. Introduction

In 1957, the priority work by S.I. Pekar [1] was published. Thirty years later, it was registered by the State Committee for inventions and discoveries at the Council of Ministers of the USSR as a domestic-science discovery “The phenomenon of propagation of additional light waves (the Pekar waves) in crystals” [2]. The essence of the discovery is contained in its formulation: “An unknown earlier phenomenon of propagation of additional light waves through crystals has been theoretically established, which is caused by the dependence of the dielectric permittivity of the crystal on the wave vector (spatial dispersion) and which consists in that, provided light waves with the frequencies close to the frequencies of exciton resonances are excited in crystals, besides ordinary birefringence waves, waves with other refractive indices

are propagated". In work [1] and other following works, new, generalized crystal optics had been created, which is relevant to exciton sections of the spectrum but includes the traditional classical optics as a particular case. The prediction of additional light waves (ALWs) and the changes to the basic laws of crystal optics were made as a result of taking into account the large effects of spatial dispersion (SD) of the dielectric permittivity of the crystal, which had been discovered for the first time. Earlier, crystal optics dealt with small SD effects only, which did not lead to the ALW emergence.

The correctness of the theoretical prediction of ALWs was beyond doubts, but it was not clear to what extent they influenced the optical characteristics of crystals and in what cases they had to be taken into account by experimenters. Owing to tremendous experimental difficulties, the answers to those questions were managed to be obtained only a lot of years later, owing to efforts of plenty of researchers.

The first experiments were executed in the late 1950s and the early 1960s at the Institute of Physics of the Academy of Sciences of the UkrSSR; here, the idea of ALWs was born and was widely discussed. In the works by Brodyn, Prikhot'ko, and others [3–6], an inconsistency between the area under the exciton absorption band and the variation range of the corresponding curve of the refractive index dispersion, i.e. the violation of the integral KKR's, was revealed for some molecular and semiconductor crystals at low temperatures. This fact, which was absolutely incomprehensible from the viewpoint of classical optics, can be explained at length in the framework of Pekar's theory, where it immediately comes from. In works by Brodyn and Pekar [7] and Gorban and Timofeev [8], the intensity oscillations of light transmitted through anthracene or  $\text{Cu}_2\text{O}$  crystals with the variation of those crystals' thickness were observed; the oscillations were explained as a result of interference between the additional and the main wave. Very important theoretical and experimental researches of the ALWs were carried out by Hopfield and Thomas in work [9] published in 1963. The results of this first stage of studies were summarized in the monograph by Agranovich and Ginzburg [10], where it was stated that "the influence of SD is small in most cases and, leaving gyrotropy aside, can be registered under rather specific conditions".

The second stage of the ALW discovery spanned the 1970s and the early 1980s, when, in a number of works carried out with the application of various experimental techniques, the existence of Pekar waves in exciton spectral sections and at low temperatures was irrefutably

proved, and their role in the changes introduced to the basic laws of crystal optics was elucidated. The results of some of those works were included into the second edition of monograph [10]; they were also expounded in detail in the collection of reviews [11]. An outcome of the long-term work of S.I. Pekar became monograph [12] published in 1982. In this monograph, the results of the ALW theory development obtained by that time were generalized; the experimental results, which were considered by the author of the discovery as its convincing confirmation, were also quoted. SD was analyzed in the books by Knox [13] and Davydov [14] and in the collective monograph "Cryocrystals" [15]. After the works cited above had already been published, in works [16, 17], two identically polarized light waves induced by a laser beam transmission through a wedged CdS crystal at a temperature of 1.8 K [18] were managed to be observed.

Therefore, it can be adopted that, by the early 1990s, the correctness of the predictions given by S.I. Pekar's theory had been completely confirmed experimentally. Practically all experiments proposed by S.I. Pekar as early as in 1958 had been carried out, as well as additional experiments which were devoted to the study of dispersion, nonlinear phenomena, and luminescence. It should be emphasized that all the proofs of the ALW existence were obtained at low temperatures and using perfect single-crystalline three-dimensional specimens, the structure of which was close to ideal, i.e. using monostructures.

During last decades, the interest of researchers became mainly concentrated in the nanophysics area direction; the objects of concern became media with quantum wells, wires, and dots, superlattices, photon crystals, and so on. In low-dimensional heterostructures, the wave vector ceases to be a continuous quantum number in the direction perpendicular to the structure plane, which, as a rule, is the direction of light propagation; therefore, the SD effects should not manifest themselves, and they did not attract enough attention really. Only during recent years, owing to the improvement of the quality of grown objects and in connection with the emergence of new physical problems, the interest to studying the non-local response of those media at their interaction with light became renewed. A new stage of investigations of SD effects in more complicated systems, which are very promising for practical applications and technical use, has started.

Because of a large time gap between the researches executed at the peak of interest in ALWs and at the present time, the sequence in the development of

this scientific direction becomes sometimes violated, and some facts that have already been established become forgotten. Therefore, challenging seems a task to summarize the results obtained for three-dimensional media on the basis of using single crystals. In particular, the following questions are to be answered: How does the additional wave influence the optical properties of three-dimensional media? In what experiments has it to be taken into consideration? and How does a consistent transition to single-wave crystal optics happen? The answers to those questions will help us to reveal common features in and differences between ALW manifestations in simple and involved systems, where SD has to be taken into account along with the quantization of energy levels associated with the spatial confinement of exciton motion.

Since the literature devoted to SD is very large (see, e.g., the monographs and collective monographs cited above), this review should be considered as a complementary one. In the first place, attention is focused on works, where it has been reliably proved and evidently demonstrated that only Pekar's theory correctly describes optical properties of crystals in the exciton spectral ranges and at low temperatures, while the use of formulas of classical single-wave crystal optics could result in crude errors. Owing to an extreme confinement put onto the review's length, only the basic directions of contemporary researches have been included for consideration.

## 2. Fundamentals of Pekar's Theory and Single-wave Optics

### 2.1. Spatial dispersion. Pekar's theory

The classical theory of crystal optics is based on the principles of causality and locality, i.e. the assumptions are made that the electric polarization of a medium at a given point in space is determined by the values of the electric field at the same point at the present time moment and at every previous moment. Generally, the assumption about the response locality is not correct, so that the polarization of the medium  $\mathbf{P}$  at the given point depends also on the values of electric field strength  $\mathbf{E}$  within some vicinity of this point. Strictly speaking, one may talk only about a polarizability kernel which is determined by an integral dependence of  $\mathbf{P}$  on  $\mathbf{E}$ . Respectively, a non-local linear relation between  $\mathbf{E}$  and the induction  $\mathbf{D} = \mathbf{E} + 4\pi\mathbf{P}$  in an infinite spatially

homogeneous medium looks like

$$\mathbf{D}(\mathbf{r}, t) = \mathbf{E}(\mathbf{r}, t) + 4\pi \int_0^\infty d\tau \int_{c\tau \geq \rho} f(\rho, \tau) \mathbf{E}(t - \tau, \mathbf{r} + \rho) d^3\rho, \quad (1)$$

where  $f(\rho, \tau)$  is a real tensor of the second rank, and integration is carried on over the region which is located inside a light cone "turned to the past". For plane waves,  $\mathbf{E}(\mathbf{r}, t) = \mathbf{E}_0 \exp[-i(\omega t - \mathbf{k}\mathbf{r})]$ , and, from Eq. (1), the relation  $\mathbf{D} = \varepsilon(\omega, \mathbf{k})\mathbf{E}$  follows.

Therefore, the violation of the principle of locality brings about the spatial dispersion, i.e. the dependence of the dielectric permittivity function  $\varepsilon$  on the wave vector  $\mathbf{k}$ . On the other hand, the dependence of  $\varepsilon$  on the frequency  $\omega$  is a consequence of the principle of causality. Until work [1] was published, SD was taken into consideration only when optically active media were examined [19]. In so doing, the quantity  $\varepsilon$  was represented in the form of a series in the wave-vector powers:

$$\varepsilon_{ij}(\omega, \mathbf{k}) = \varepsilon_{ij}(\omega) + i\gamma_{ijl}(\omega)k_l + \alpha_{ijlm}(\omega)k_l k_m, \quad (2)$$

where the expansion coefficients are equal, by the order of magnitude, to the size of the region of mutual influence of neighbor particles. The first term in the expansion is responsible for the appearance of a difference between the phase velocities of waves with right and left circular polarizations in media without the inversion center. It results in very small corrections to the refractive indices for visible light, of the order of  $a/\lambda \approx 3 \times 10^{-3}$ , where  $a$  is the lattice constant, and  $\lambda$  is the length of the wave in the medium; therefore, they can be called small SD effects, although the magnitude of the polarization plane rotation can be very large, provided that the thickness of the specimen is considerable. The number of waves remains the same as in the case without taking SD into account, when two waves with mutually orthogonal polarizations can propagate in the given direction  $\mathbf{k}$ . In media with the inversion center,  $\gamma(\omega) \equiv 0$ , and the SD effects are proportional to  $(a/\lambda)^2 \approx 10^{-5}$ . This term, which has not been considered earlier in crystal optics owing to its extreme smallness, is responsible, as Ginzburg showed [20], for the optical anisotropy of cubic crystals. The effect was revealed in a crystal of cuprous oxide, while studying the quadrupole transition in precision experiments by Gross and Kaplyanskii [21], and confirmed by Gorban and Timofeev [22].

In his work [1], Pekar was the first who predicted large SD effects in the range of exciton resonances. They

are associated with the collective character of electron excitations and a much larger extension of the non-locality region, which can reach the value of  $10^{-5} \div 10^{-4}$  cm under favorable conditions [12]. In this case, expansion (2), which is valid far from the resonance, turns out insufficient for SD to be taken into account in the vicinity of the resonance.

Owing to the strong exciton-photon interaction in the resonance region, “mere” excitons and photons are not real elementary excitations of the crystal; instead, these are mixed states, which were called by S.I. Pekar as photon-like excitons. Later on, Hopfield has introduced a term “polariton” [23]. In the elementary case of an isolated resonance in the exciton spectral range of the isotropic crystal, Pekar considered SD by having presented the  $\varepsilon(\omega, \mathbf{k})$ -dependence in the form

$$\varepsilon(\omega, \mathbf{k}) = \varepsilon_0 + \frac{2\pi e^2 f N / m \omega_0}{\omega_0 + \hbar \mathbf{k}^2 / 2M - \omega - i\Gamma}, \quad (3)$$

where  $\varepsilon_0$  is the background value of  $\varepsilon$ ;  $e$  and  $m$  are the electron charge and mass, respectively;  $f$  is the oscillator strength in the elementary lattice;  $N$  is the number of cells in a unit volume;  $\omega_0 = E(0)/\hbar$ ;  $E(0)$  is energy which is required for the excitation of an exciton with a zero quasimomentum; and  $M$  and  $\Gamma$  are the effective mass and the inverse lifetime of exciton, respectively. Thus, the dependence of  $\varepsilon$  on  $\mathbf{k}$  turns out to be included into the denominator, where the second term – if multiplied by  $\hbar$  – is the kinetic energy of an exciton, and non-locality is caused by the exciton motion in the band. For local excitations, e.g., for impurity centers with  $M \rightarrow \infty$ , formula (3) automatically leads to the ordinary equation of classical optics (see Eq. (14) below).

The account of SD in such a manner essentially changes the behavior of  $\varepsilon$  at  $\omega \rightarrow \omega_0$ , where the second term in the denominator becomes prevailing. Therefore, even under the condition  $a/\lambda \ll 1$  (this is the only limit, where the effective mass approximation is valid), large SD effects, i.e. large variations of  $\varepsilon$  in comparison with  $\varepsilon$  calculated taking no SD into account, manifest themselves. Since  $k = (\omega/c)\tilde{n}$  for an arbitrary fixed polarization in an isotropic crystal, where  $\tilde{n}$  is the complex refractive index, the dispersion equation  $\varepsilon(\omega, k) = \tilde{n}^2$  becomes a quadratic one with respect to  $\tilde{n}$  and determines two values for every frequency  $\omega$ :

$$\tilde{n}_{\pm}^2 = \frac{1}{2}(\mu + \varepsilon_0) \pm \sqrt{\frac{1}{4}(\mu - \varepsilon_0)^2 + b}, \quad (4)$$

where

$$\mu = \mu' + i\mu'', \quad \mu' = \frac{2Mc^2}{\hbar\omega_0^2}(\omega - \omega_0),$$

$$\mu'' = \frac{2Mc^2}{\hbar\omega_0^2}\Gamma, \quad b = \frac{4\pi c^2 M e^2}{\hbar\omega_0^3 m} N f.$$

Dispersions of the refractive indices for photon-like excitons, calculated by formula (4) in an idealized case where damping is absent ( $\Gamma = 0$ ), are depicted in Fig. 1 for a positive (panel *a*) and a negative (panel *b*) effective mass of exciton (in every figure, here and below, the energy  $\hbar\omega$  is given in units of the wave number  $\nu = 1/\lambda_0$  cm $^{-1}$ , where  $\lambda_0$  is the light wavelength in vacuum). Solid curves describe the “+”- and “-”-waves (following Pekar’s terminology) and correspond to the root values of Eq. (4) taken with the sign plus and minus, respectively. In contrast to the classical theory of birefringence, where the dispersion branches – they are plotted in Fig. 1 by dashed curves – have vertical asymptotes, the asymptotes in Pekar’s theory are inclined, whence the availability of two solutions for every frequency  $\omega$  becomes evident. While moving away from the resonance, one of the waves becomes asymptotically transformed into an ordinary wave of classical crystal optics, and the other fades down, because its amplitude becomes very small.

The two waves are identically polarized and propagate in the same direction, but with different velocities (with different  $\tilde{n}$ ’s). It is their principal difference from two waves arising in an anisotropic crystal owing to birefringence, which also have different  $\tilde{n}$ ’s but are polarized orthogonally to each other. The two identically polarized waves are transverse (below, they will be designated by index *T*), i.e.  $\mathbf{E} \perp \mathbf{k}$  for them, and their dispersion equations look like  $\varepsilon(\omega, \mathbf{k}) = (c\mathbf{k}/\omega)^2$ . In work [1], a possibility for strictly longitudinal waves (they will be designated by index *L*) to propagate was also demonstrated; for those waves,  $\mathbf{E} \parallel \mathbf{k}$ , and they comprise a macroscopic field of a moving exciton. The longitudinal waves are the solutions of the equation  $\varepsilon(\omega, \mathbf{k}) = 0$ . According to Pekar’s theory, the exciton wave transforms into an additional light one owing to the electromagnetic field accompanying it; therefore, the number of transverse ALWs is equal to the number of excitons which undergo a resonance.

In connection with the appearance of ALWs, Maxwell boundary conditions – the continuity of the tangential components of the vectors  $\mathbf{E}$  and  $\mathbf{H}$  across the interface between two media – turned out insufficient for the determination of the amplitudes of the reflected and transmitted waves from the amplitude of the incident one. This is why Pekar has introduced an additional

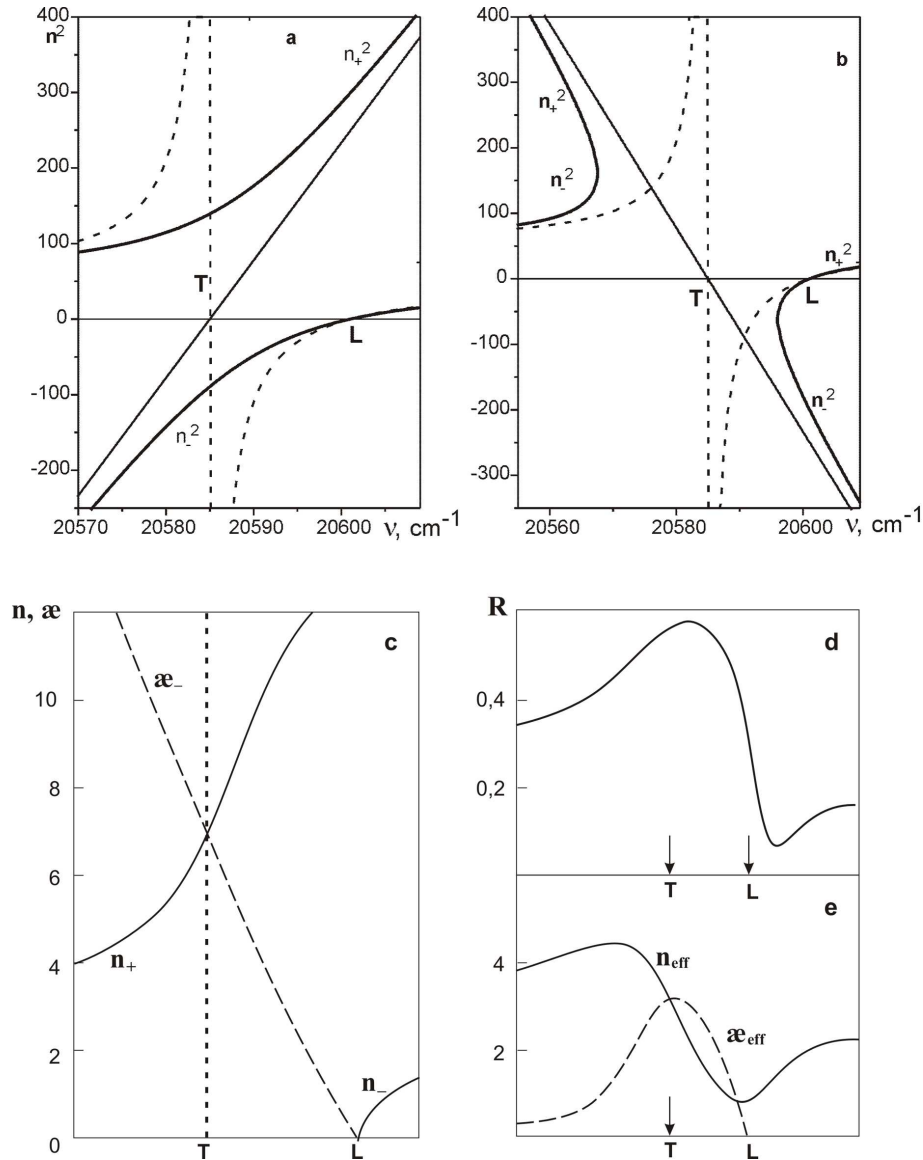


Fig. 1. *a* – dispersion of the refractive indices for photon-excitons calculated in the framework of Pekar’s (solid curves) and classical (dashed curves) theories for an isotropic crystal and an isolated resonance for the positive effective mass of an exciton. *b* – the same as in panel *a*, but for the negative effective mass of an exciton. *c* – the dependences  $n_+(\omega)$ ,  $n_-(\omega)$ , and  $\kappa_-(\omega)$  for  $M > 0$ . *d* – spectrum of light reflection from semiinfinite crystal  $R$ , calculated for the effective quantities  $n_{\text{eff}}(\omega)$  and  $\kappa_{\text{eff}}(\omega)$  (panel *e*). The main parameters of calculations correspond to those of  $A_{n=1}$ -exciton in a CdS crystal:  $\Delta_{LT} = 16 \text{ cm}^{-1}$ ,  $\omega_0 = 20585 \text{ cm}^{-1}$ ,  $\varepsilon_0 = 7.4$  (except for panels *a* and *b*, for which  $\varepsilon_0 = 50$  to make the growth of the photon-exciton branch above the frequency  $\omega_L$  evident);  $M = 0.8m_e$  (panels *a*, *c*, *d*, and *e*) and  $-0.8m_e$  (panel *b*);  $\Gamma = 0$

boundary condition (ABC)

$$\mathbf{P}_{\text{ex}}(\mathbf{r}) = 0 \tag{5}$$

at the crystal surface, where  $\mathbf{P}_{\text{ex}}$  is the exciton portion of crystal polarization. In this case, the crystal surface is a node surface for both exciton waves and the specific

exciton dipole moment. Condition (5) means that an exciton wave is specularly reflected from the surface.

Using this ABC and considering the opportunity for both the transverse and longitudinal waves to propagate, Pekar has derived new generalized formulas for a light wave reflected from a crystal in the exciton spectral

range. The problem concerning the transmission of light through and its reflection from a plane-parallel plate was also solved. The results of researches devoted to the influence of the crystal surface on the solutions obtained for an infinite crystal testified that there is a possibility of the existence of surface exciton states. One of the most important results of Pekar's theory became a conclusion about the opportunity for the universal KKR's to be inapplicable in the range of exciton resonance and at low temperatures. Thus, new generalized crystal optics has been created.

## 2.2. Classical crystal optics

For making a comparison between the experimental and theoretical results, it is necessary to concisely recall the formulas and laws of classical crystal optics. An isotropic medium is characterized by a complex dielectric permittivity  $\varepsilon = \varepsilon' + i\varepsilon'' = \tilde{n}^2$  and a complex index of refraction  $\tilde{n} = n + i\kappa$ , where  $n = \text{Re } \tilde{n}$  is the ordinary refractive index, and  $\kappa = \text{Im } \tilde{n}$  is the absorption coefficient;  $\varepsilon' = n^2 - \kappa^2$ ; and  $\varepsilon'' = 2n\kappa$ . The parameter  $\kappa$  characterizes the damping of the amplitude and, therefore, the intensity  $I$  of a light wave as it propagates in the medium. The change of the light intensity  $I$  from the point  $z = 0$  to the point  $z = d$  is described by the *Bouguer-Lambert law*  $I(d) = I(0) \exp(-4\pi\kappa d/\lambda_0)$ . Energy absorption is determined by the imaginary part of the dielectric permittivity,  $\varepsilon''$ .

If the frequency dependences of  $n$  and  $\kappa$  are known, one can use the Fresnel formulas to calculate the spectral dependences of the reflection coefficient of the crystal,  $R$ , and the phase variations of a light wave at its reflection,  $\Delta\varphi$ . In the case of normal incidence,

$$R(\omega) = \frac{[n(\omega) - 1]^2 + [\kappa(\omega)]^2}{[n(\omega) + 1]^2 + [\kappa(\omega)]^2}, \quad (6)$$

$$\text{tg } \Delta\varphi(\omega) = \frac{2\kappa(\omega)}{[n(\omega)]^2 + [\kappa(\omega)]^2 - 1}. \quad (7)$$

In classical crystal optics, where only the frequency dependence of the dielectric permittivity  $\varepsilon(\omega)$  is taken into account, the real and imaginary parts are coupled by the integral KKR's

$$\varepsilon'(\omega) = 1 + \frac{1}{\pi} \int_{-\infty}^{\infty} \frac{\varepsilon''(x)}{x - \omega} dx, \quad (8)$$

$$\varepsilon''(\omega) = -\frac{1}{\pi} \int_{-\infty}^{\infty} \frac{\varepsilon'(x) - 1}{x - \omega} dx. \quad (9)$$

Here, the principal values of integrals are meant. If the band is isolated enough, relation (8) can be rewritten in the form

$$\varepsilon'(\omega) = \varepsilon_0 + \frac{1}{\pi} \int \frac{\varepsilon''(x)}{x - \omega} dx, \quad (10)$$

where  $\varepsilon_0$  is a contribution to  $\varepsilon'$  made by all other transitions, except for that under consideration, and the integration over  $x$  is carried out only within the limits of a given band. According to Eq. (10), in the middle of the band range, where absorption is substantial, the refractive index  $n$  has to fall down with growing  $\omega$ , i.e. there must be a section of abnormal dispersion. Really, if  $\omega$  is located towards long waves from the absorption range, the value of the integral in Eq. (10) is positive, because  $\varepsilon''(x) \geq 0$  and  $x - \omega > 0$  within the actual interval of integration. At the same time, if  $\omega$  is located towards short waves from the absorption range,  $x - \omega < 0$ , and the value of the integral is negative.

If  $\omega$  is located far enough from the center of the absorption band, then Eq. (10) yields

$$n^2(\omega) = \varepsilon_0 + \frac{A}{\omega_1 - \omega}, \quad (11)$$

where

$$A = \frac{1}{\pi} \int \varepsilon''(\omega) d\omega \quad (12)$$

is the integral over the band, and  $\omega_1$  is a definite fixed frequency. It becomes evident that the strength of the transition oscillator (it is a multiplier of the constant  $A$ ) can be determined by two independent methods: (i) from the curvature of the dispersion curve far from the absorption range and (ii) from the area under the absorption curve. Both methods of measurements are really applied in practice.

At last, we would like to present the final relations for a model of the medium which absorbs as a collection of classical oscillators; such a model is widely used, and the relations between  $\varepsilon'$  and  $\varepsilon''$  become substantially simpler in this case. In the frequency interval near an isolated resonance,

$$\varepsilon(\omega) = \varepsilon_0 + \frac{(4\pi N e^2 / m) f}{\omega_0^2 - \omega^2 - i\omega\gamma}. \quad (13)$$

The difference between squared frequencies can be presented in this case as  $\omega_0^2 - \omega^2 = (\omega_0 - \omega)(\omega_0 + \omega) \approx 2\omega_0(\omega_0 - \omega)$ . Then, from Eq. (13), an approximate relation

$$\varepsilon(\omega) = \varepsilon_0 + \frac{A}{\omega_0 - \omega - i\Gamma} \quad (14)$$

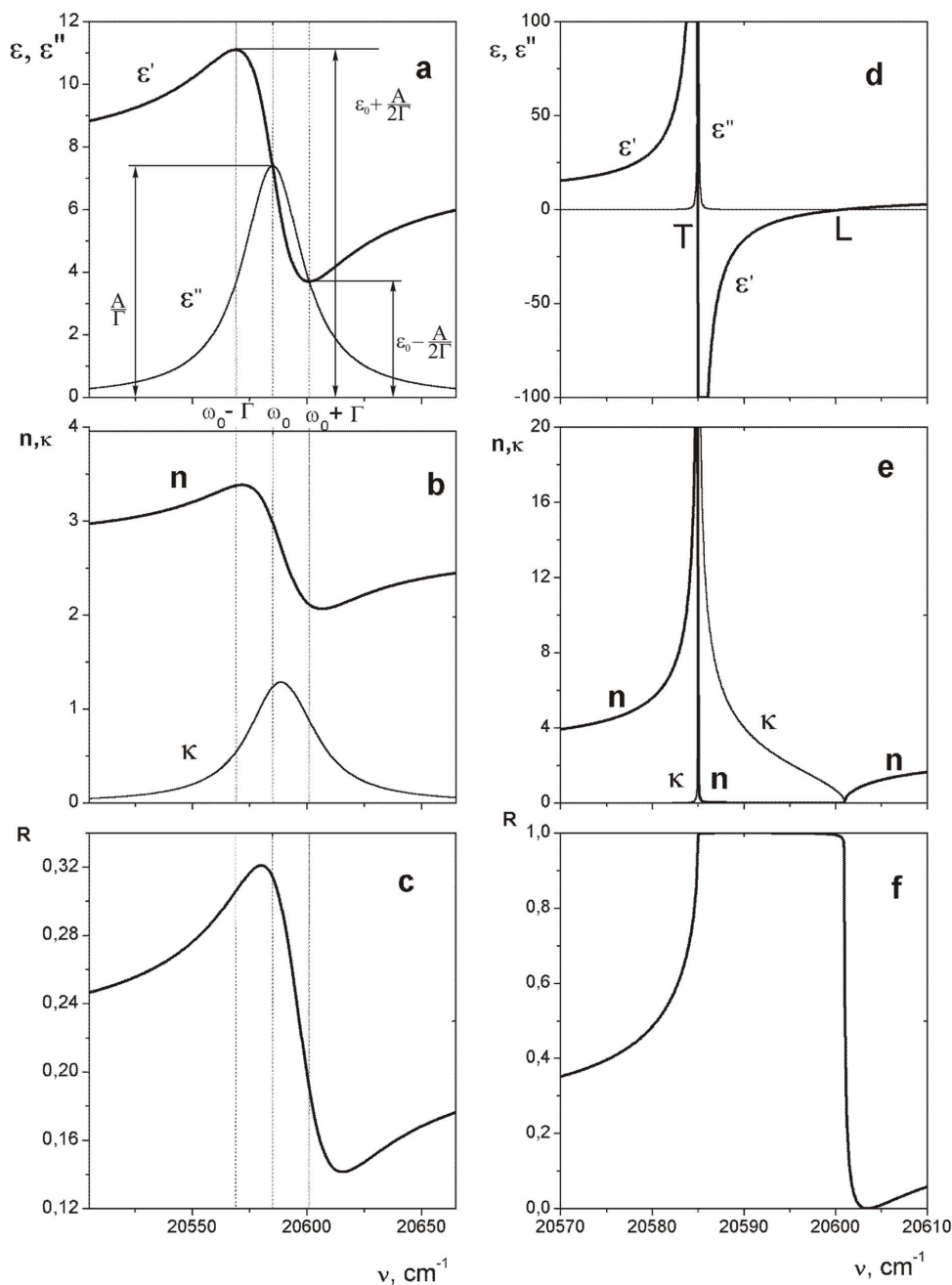


Fig. 2. Optical characteristics  $\epsilon'(\omega)$  and  $\epsilon''(\omega)$  (panels *a* and *d*),  $n(\omega)$  and  $\kappa(\omega)$  (panels *b* and *e*), and  $R(\omega)$  (panel *c* and *f*) of a classical oscillator for various values of  $\Gamma = \Delta_{LT}$  (panels *a*, *b*, and *c*) and  $4 \times 10^{-4} \Delta_{LT} (\approx 0)$  (panels *d*, *e*, and *f*). The parameters of calculations are the same as in Fig. 1, *c*, but  $M = \infty$  and  $\Gamma \neq 0$

follows, where  $A = 2\pi N e^2 f / (m\omega_0)$ , and  $\Gamma = \gamma/2$ . The real and imaginary parts of  $\epsilon$  look like

$$\epsilon'(\omega) = \epsilon_0 + \frac{A(\omega_0 - \omega)}{(\omega_0 - \omega)^2 + \Gamma^2} \quad (15)$$

and

$$\epsilon''(\omega) = \frac{A\Gamma}{(\omega_0 - \omega)^2 + \Gamma^2}, \quad (16)$$

respectively. The plots of these functions are depicted in Fig. 2, *a*. The figure demonstrates that the absorption

curve has a symmetric Lorentzian shape with a halfwidth  $H = 2\Gamma = \gamma$ . The dispersion curve has a typical shape with the section of anomalous dispersion, and the points where it becomes maximal ( $\varepsilon'_{\max} = \varepsilon_0 + A/2\Gamma$ ) and minimal ( $\varepsilon'_{\min} = \varepsilon_0 - A/2\Gamma$ ) correspond to the frequencies ( $\omega_0 - \Gamma$  and  $\omega_0 + \Gamma$ ) which are used to determine the halfwidth of the absorption band. The amplitude of curve variation,  $\varepsilon'_{\max} - \varepsilon'_{\min}$ , is precisely equal to the maximal absorption at the resonance frequency ( $\varepsilon'_{\max} = A/\Gamma$ ).

Very interesting is the idealized case  $\Gamma = 0$  depicted in Fig. 2,*d* and corresponding to dashed curves in Figs. 1,*a* and *b*. If  $\varepsilon = 0$ , the excitation of longitudinal oscillations in the medium with the frequency  $\omega_L$  becomes possible; for these oscillations,  $\mathbf{E} \parallel \mathbf{k}$ , but the group velocity equals zero, because  $\omega_L$  is independent of  $\kappa$ . From Eq. (14), it becomes obvious that  $\omega_L = \omega_0 + A/\varepsilon_0$ . The dispersion branches tend to  $\pm\infty$ , if  $\omega \rightarrow \omega_0 \equiv \omega_T$ ; the limit values of  $\varepsilon$  remain the same as those in the presence of damping; namely, the low-frequency one  $\varepsilon(0) = \varepsilon_0 + (4\pi N e^2 f / m \omega_0^2)$ , which follows from Eq. (13), and the high-frequency one  $\varepsilon(\infty) = \varepsilon_0$ . In the region of longitudinal-transverse splitting (in the vicinity of  $\Delta_{LT} = \omega_L - \omega_0 = A/\varepsilon_0$ ), the quantity  $\varepsilon' < 0$  (Fig. 2,*d*), which corresponds to a purely imaginary refractive index:  $n = 0$  and  $\kappa \neq 0$  (Fig. 2,*e*). In this case, the wave amplitude falls down exponentially in the crystal and does not oscillate in space, because  $\mathbf{k}'\mathbf{r} = (\omega/c)\mathbf{n}\mathbf{r} = 0$  ( $\mathbf{k} = \mathbf{k}' + i\mathbf{k}''$ ). According to relation (6), a semiinfinite medium must totally reflect the incident energy in this case, i.e.  $R = 1$  (Fig. 2,*f*). True absorption, which is formally described by the area under the  $\varepsilon''(\omega)$ -curve, tends at  $\Gamma \rightarrow 0$  to a  $\delta$ -function located about the frequency  $\omega_0$  (Fig. 2,*d*) and approaches the limit of  $2\pi^2 N e^2 f / (m \omega_0)$ . It should be emphasized that the limit is not equal to zero. The same area is contained under the Lorentzian curve at  $\Gamma \neq 0$  (see Fig. 2,*a*).

Note that, since  $A = \Delta_{LT}\varepsilon_0$ , relation (3) is often written down in the following form:

$$\varepsilon(\omega, \mathbf{k}) = \varepsilon_0 + \frac{\Delta_{LT}\varepsilon_0}{\omega_0 + \hbar k^2/2M - \omega - i\Gamma};$$

then

$$b = \frac{2Mc^2}{\hbar\omega_0^2} \Delta_{LT}\varepsilon_0 \quad (17)$$

in solution (4).

The considered case  $\Gamma = 0$  is an illustration of strong exciton-photon mixing without taking SD into account. One can see that there is a strong repulsion between

dispersion branches in this case at a point, where the “mere” exciton and photon branches intersect each other, i.e. a strong polariton effect of exciton-photon mixing is observed, but ALWs do not emerge. The spectrum of polaritons in the framework of the classical theory of light dispersion for infrared frequencies has been found for the first time by Tolpygo [24]. Nowadays, the term “polariton” is used in case of substantial SD as well.

Before proceeding to the discussion of experimental confirmations of Pekar’s theory, it should be noted that the ALW manifestations in various crystals depend on the relations between the parameters of a specific exciton transition. The most important among them are the oscillator strength, which governs the longitudinal-transverse splitting  $\Delta_{LT}$  and characterizes the strength of exciton-photon interaction; the effective mass  $M$ , which determines the slope of the asymptote in Figs. 1,*a* and *b*; and the damping constant  $\Gamma$ , which governs the exciton-phonon coupling. The case, where the values of the refractive index for ALWs at frequencies lower than the longitudinal frequency  $\omega_L$  are not very much yet, is most favorable; it can be realized provided that the value of  $M$  is minimal, the value of  $\Delta_{LT}$  is not very large, and the value of  $\Gamma$  is very small.

Historically, it happened that a very large body of experimental confirmations of Pekar’s theory was obtained making use of CdS crystals. They turned out to be a good model object with a favorable relation for the parameters of the lowest exciton, which provided an opportunity to observe ALWs using various optical methods. That is why the features of manifestations of additional waves are considered here using just this crystal as an example.

From Fig. 1,*a*, one can see that the frequency  $\omega_L$  splits the frequency range into two spectral intervals, in which the manifestations of the additional wave differ in principle. Above  $\omega_L$ , both waves have positive values of  $\tilde{n}^2$ , i.e. their refractive indices are real and they can pass through a crystal without being absorbed. Below  $\omega_L$ , we have  $\tilde{n}^2 > 0$  for the “+”-wave, so that it can be transmitted through a crystal without absorption, but  $\tilde{n}^2 < 0$  for the “-”-wave, which means that  $n_- = 0$  and  $\kappa_- \neq 0$  (see Fig. 1,*c*). In the framework of classical optics, as was shown above, the latter wave must be completely reflected by the crystal; therefore, the medium does not absorb energy at all in the idealized case  $\Gamma = 0$ . Since the characteristic features of manifestations of additional waves are different in those two cases, we consider first the experiments which confirmed the ALW existence in the spectral interval above and then below  $\omega_L$ .

### 3. Manifestations of Additional Waves at Frequencies above $\omega_L$

The first convincing proofs of the existence of an additional wave in the spectral range above  $\omega_L$  were obtained in experiments dealing with Fabry–Perot interference in thin crystals. Later on, they were also obtained in a series of works devoted to the Mandelshtam–Brillouin scattering, measurements of the picosecond laser pulse transit time, and, at last, in works on light refraction by wedge-shaped CdS crystals. The results of three first groups of researches were described in detail in monographs [10–12]. Therefore, we consider some basic features of those works only in brief, in order to analyze the experiments on the light refraction by a wedge-shaped crystal in more details.

#### 3.1. Interference spectra of thin crystals

In works [25–29], the reflection and absorption spectra of high-quality superthin plane-parallel CdSe and CdS crystals at temperatures of 4.2 and 1.6 K were studied. In these spectra, clearly distinguished was a Fabry–Perot interference structure that corresponded to the condition

$$2dn = N\lambda, \quad (18)$$

where  $d$  is the crystal thickness,  $\lambda$  the light wavelength in vacuum, and  $N$  an integer number (the order of interference). Below the frequency  $\omega_L$ , when only the “+”-wave can propagate through the crystal, this structure has a single-period character, which correlates with the variation of  $n_+(\omega)$ . Above the frequency  $\omega_L$ , when both the “+”- and “-”-waves can freely propagate through the crystal, the structure of the spectrum is characterized by two periods of oscillations: the oscillations with a large amplitude and a larger period correspond to the Fabry–Perot interference of the “-”-wave; they interfere with oscillations with a small amplitude and a small period, which are the manifestation of the Fabry–Perot interference of the “+”-wave.

On the basis of the measured spectral positions of interference extrema and crystal thicknesses, the authors of works [25–29] evaluated the parameters of the theory and calculated both the dispersion of polariton branches and the reflection spectra of crystalline plates. In all cases, the agreement between the experimentally measured spectra and the spectra theoretically calculated in the framework of Pekar’s theory was excellent. The results of those works are summarized and discussed at length in monograph [12].

#### 3.2. Mandelshtam–Brillouin resonance scattering

For the first time, the light scattering by acoustic phonons, taking ALWs into account, was examined theoretically in work [30]. A laser beam with frequency  $\omega$  and wave vector  $k$  was considered to propagate into the crystal depth normally to the crystal surface ( $k > 0$ ). The beam was scattered in all directions, but theoretically was considered only light that was reflected by the crystal into vacuum normally to the crystal surface ( $k < 0$ ). In the course of scattering, the energy and momentum conservation laws,

$$\omega' = \omega + \Delta\omega \quad (19)$$

and

$$k' = k - |\Delta\omega|/V, \quad (20)$$

respectively, are satisfied, where  $\omega'$  and  $k'$  are the frequency and the wave vector, respectively, of the scattered photon;  $\hbar|\Delta\omega|$  is the energy of a phonon that participates in the scattering;  $V$  the sound velocity; and  $|\Delta\omega|/V$  the modulus of the phonon’s wave vector. At the Stokes scattering, the elementary event of scattering is accompanied by the phonon emission, and  $\Delta\omega < 0$ ; at the antiStokes one, a phonon is absorbed, and  $\Delta\omega > 0$ .

Provided that the polariton dispersion branches and the sound velocity are known, one can calculate the frequency shift  $\Delta\omega$  for every initial frequency  $\omega$ . At  $\omega < \omega_L$ , an ordinary Stokes–anti-Stokes doublet, which corresponds to jumps between the states of the  $n_+$ -branch (from states with  $k > 0$  into states with  $k < 0$ ), is to be observed in the scattered light. If  $\omega > \omega_L$ , another three Stokes and three anti-Stokes peaks corresponding to jumps between  $n_+$ - and  $n_-$ -branches should appear in the spectrum of scattered light.

Starting from 1977, experiments on the Mandelshtam–Brillouin resonance scattering (MBRS) have been carried out for a number of crystals: GaAs, CdTe, CdS, ZnSe, HgJ<sub>2</sub> [31–34]. In all cases, the emergence of additional scattering peaks in the resonance region has been registered. The number of additional satellites can be more than three, if the structure of exciton bands is more complicated than that corresponding to Fig. 1 (the presence of heavy- and light-exciton bands), as well as because scattering can occur not only by longitudinal acoustic (LA) but also by transverse acoustic (TA) phonons. A detailed statement of the MBRS theory and the experimental

results are given in Koteles's review [11]. Thus, ALWs manifest themselves in scattering spectra by means of the emergence of additional satellites near the frequency of primary light, if  $\omega > \omega_L$ .

### 3.3. Direct measurements of the group velocity of light waves

In work [35], the transit time of a picosecond laser pulse was measured for its passage through a CuCl crystalline plate, and the time of delay was used to determine the group velocity  $V_g$ . The results obtained were compared with those calculated from the dispersion curves.

Only the pulse of the “+”-wave with a frequency below  $\omega_L$  was shown to be transmitted through the crystal. Moreover, in accordance with theoretical calculations, at a frequency where the  $n_+(\omega)$ -dependence had an inflection point, the group velocity  $V_g$  was found to slow down by more than three orders of magnitude. The “-”-wave was observed only above  $\omega_L$ , and its  $V_g$  proved to be in good agreement with values calculated from the  $n_-(\omega)$  dependence. But the most important fact was that two pulses with identical polarizations and frequencies (in the vicinity of  $\omega_L$ ) but separated in time were managed to be registered at the plate's output, whereas only one pulse had fallen onto the plate's surface. This was a direct proof of the existence of an additional wave in a CuCl crystal.

### 3.4. Light refraction by a wedge-shaped crystal

The results of experiments dealing with the light transmission through a wedge-shaped crystal appeared the most straightforward proof of the ALW existence. As early as in 1958, S.I. Pekar suggested to make such an experiment due to its theoretical transparency, visualization, and maximal persuasiveness [36]. For the first time, this method was applied by Broser et al. in 1981 to study excitons in CdS [37], but, owing to large systematic difficulties (in particular, strong absorption), the authors were not succeeded in registering the simultaneous transmission of two identically polarized waves. The maximal among other measured values of the refractive index,  $n \approx 6.4$ , was observed at a frequency of approximately  $\omega_T$ , which is far from  $\omega_L$  that starts the interval where two waves could propagate simultaneously. The problem was solved only in 1984 [16]. A theoretical consideration of the light transmission through an absorbing prism taking ALWs into account was made in work [38]. The relevant experiment was described in detail in work [39].

In works [16, 39], a CdS crystal with an average thickness of  $0.5 \mu\text{m}$  and a refraction angle of  $50''$  was studied at a temperature of 1.8 K. The light source was a tunable dye laser on dye with a spectral width of about  $0.3 \text{ \AA}$ . The specific power was lower than  $10^{-4} \text{ W/cm}^2$ , so that nonlinear variations of the refractive index could be neglected. Measurements were carried out at light polarization  $\mathbf{E} \perp \mathbf{C}$ , where  $\mathbf{C}$  is the optical axis of the crystal, and two parallel polarizers – located before and behind the crystal – were used for the best polarization extraction. The specimen was illuminated with a collinear light beam about  $1 \text{ mm}^2$  in cross-section. The beam deflected by the crystal was focused in the focal plane of a lens into a spot about  $15 \mu\text{m}$  in diameter. The spot displacement was monitored visually by means of a measuring microscope. Photo-electric registration with the help of an OMA-2 optical multichannel analyzer allowed the spot intensity to be controlled as well. To enhance the accuracy of angular measurements, the latter were carried out at a large angle of incidence  $\theta = 55.5^\circ$ .

While the laser frequency was varied in the interval of  $\omega$  lower than  $\omega_L$  of  $A_{n=1}$ -exciton, a single bright spot corresponding to the “+”-wave was observed. As the laser frequency approached  $\omega_L$ , this spot faded out and became more and more shifted in the visual field of a microscope (see Fig. 3, *a*). Starting from the frequency  $\omega_L$ , a second spot appeared, which corresponded to the “-”-wave and whose intensity quickly grew as  $\omega$  increased. In a certain frequency region, two spots were observed simultaneously; in this case, they had identical frequencies  $\omega$  and polarizations of the vector  $\mathbf{E}$ . Careful measurements in the frequency range  $\omega < \omega_L$  allowed another, substantially weaker spot to be registered, whose angle of deviation was three times as large as the deviation angle of the first spot. The third spot corresponded to a triple transmission of the “+”-wave through the wedge as a result of the reflection from its surfaces. Being reduced by a factor of three, these displacements fitted well the dependence  $l(\lambda)$  for light passed through the wedge only once.

The experimentally measured displacements of the laser beam were used to calculate the dispersion of the refractive index; the corresponding calculation results are plotted by dots in Fig. 3, *b*. On the basis of the data obtained, the parameters of Pekar's theory ( $\varepsilon_0$ ,  $M$ ,  $\Delta_{LT}$ , and  $\Gamma$ ) were determined, and the dependences  $n_+(\omega)$  and  $n_-(\omega)$  were calculated (they are depicted by the solid and the dashed curve, respectively, in the same figure). An agreement between the theory and the experiment proved to be quite good.

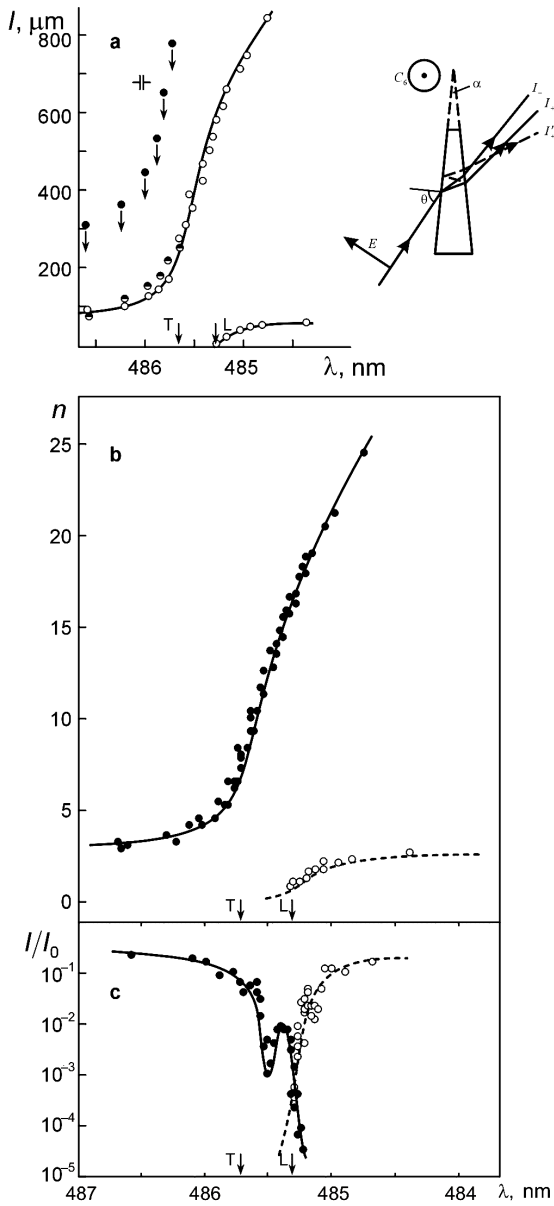


Fig. 3. *a* – dependence of the spot displacement in the focal plane on the incident light wavelength (circles); points correspond to the displacements of the spot of the “+”-wave, transmitted three times through the prism (see beam  $I_+$  in the inset); semisolid circles correspond to the previous dependence reduced by a factor of three. *b* – experimentally measured dispersion of the refractive indices  $n_+$  (points) and  $n_-$  (circles); theoretical curves for the same quantities (solid and dashed curve, respectively) calculated by Pekar’s formulas. *c* – relative transmission coefficient for the “+”- (points) and “-”-waves (circles) on logarithmic scale; the curves are eye guides drawn through experimental points.  $T$  and  $L$  are the positions of transverse and longitudinal excitons, respectively [16, 39]

Owing to the spatial separation of the “+”- and “-”-waves, their transmission spectra were managed to be measured for the first time (Fig. 3,*c*). The figure demonstrates that the envelope of the partial transmission curves for the “+”- and “-”-waves has a two-humped shape and is similar to the transmission curves for a plane-parallel thin crystal (see Fig. 4,*b*). In the framework of Pekar’s theory, a complicated shape of the absorption curve, provided that the exciton band is simple and parabolic, can be explained by the fact that, besides the absorption coefficients of each waves ( $\kappa_{\pm}$ ), the shape also depends on the spectral dependence of the ratio between the amplitudes of those waves at the moment when the latter are excited by light incident on the crystal. A better agreement between the experiment and the theory was obtained after the frequency dependence of the damping constant  $\Gamma(\omega)$  had been taken into account [39, 40].

#### 4. Manifestations of Additional Waves below the Frequency $\omega_L$

As was already emphasized above, the manifestations of an additional wave are implicit and veiled in this spectral interval. Therefore, they can be observed only in the course of simultaneous researches of all optical characteristics of the crystal, namely, the dispersion of the refractive index, the transmission and reflection spectra.

##### 4.1. Violation of KKR’s

As early as in his first works dealing with additional waves, Pekar put forward a new viewpoint concerning the exciton absorption of light. According to works [1, 36], this absorption “originates from the transitions of the system from the exciton states created by light into any other states, except for the initial ones. If those transitions are accompanied by light emission, the Raman scattering of the primary light takes place. If those transitions are thermally induced and are accompanied by the excitation of thermal vibrations, an ordinary light absorption takes place”. Thus, absorption is associated with a finite lifetime of an exciton with respect to radiationless transitions. If there are no such transitions, absorption is absent as well, whatever large the oscillator strength is. S.I. Pekar repeatedly emphasized that if SD of  $\varepsilon$  is essential, the oscillator strength of exciton transition should be determined making use of the curvature of the refractive index dispersion curve only, rather than the area under the

absorption curve. Actually, this means that KKR's are violated.

The first experimental evidence that these relations may be invalid in the range of exciton absorption at low temperatures was obtained in works [3–6] which have demonstrated that the amplitude of variation of the refractive index dispersion curve  $n(\omega)$  is always larger than the maximal coefficient of absorption  $\kappa_{\max}$ . The problem was solved more comprehensively and in a wider scope, when the spectrum  $\kappa(\omega)$  was managed to be measured reliably [41], and the behavior of the curve  $n(\omega)$  was determined within the whole absorption band interval rather than only in its “wing” sections. In the work by Brodin, Davydova, and Strashnikova [42], the dependence  $n(\omega)$  for a CdS crystal 0.33  $\mu\text{m}$  in thickness and at a temperature of 4.2 K was obtained for the first time by the straightforward method of measuring the phase of the transmitted wave. It turned out that, within the halfwidth  $H$  of the  $A_{n=1}$ -exciton absorption band, *no anomalous section was observed*, whose presence is obligatory if KKR's are satisfied. The refractive index steadily increased as the frequency grew up to the longitudinal one, and the general profile of the experimentally measured dispersion curve completely corresponded to the theoretical one (see Fig. 1, *c*). In work [43], it was shown that the variation range of the curve  $n(\omega)$  is about an order of magnitude larger than the  $\kappa_{\max}$ -value measured in work [41].

#### 4.1.1. Comparison of the dependences calculated by KKR's and measured experimentally

**A.** The real and imaginary parts of the complex refractive index  $\tilde{n}$ , i.e.  $n$  and  $\kappa$ , are also coupled with each other by integral relations [44–46]

$$n(\omega) = 1 + \frac{2}{\pi} \int_0^{\infty} \frac{x\kappa(x)dx}{x^2 - \omega^2}, \quad (21)$$

$$\kappa(\omega) = -\frac{2\omega}{\pi} \int_0^{\infty} \frac{n(x)dx}{x^2 - \omega^2}. \quad (22)$$

On the basis of the absorption spectrum  $\kappa(\omega)$  in the range of  $A_{n=1}$ - and  $B_{n=1}$ -exciton states (curves 1 in Figs. 4, *a* and *b*) experimentally measured in work [41] and making use of formula (21), one can calculate the dispersion of the refractive index  $n(\omega)$  (curves 3) and compare it with that measured experimentally in works [16, 42] (curves 2). (Figure 4, *b* depicts the

lower part of Fig. 4, *a*, scaled up.) As is seen from the figure, the calculated dependence contains sections of anomalous variation of  $n(\omega)$  located within the width intervals of absorption bands, and the ranges of variation are approximately equal to the maximal values  $\kappa_{\max}$ . At the same time, all the curves  $n(\omega)$  measured by various methods in works [16, 28, 42] revealed no anomalous sections in the range of  $A_{n=1}$ -exciton, and their ranges of variation were substantially larger than  $\kappa_{\max}$ . But the most important fact was the experimental registration of simultaneous transmission through the crystal of two waves with different  $n$ 's, whereas relation (21) brings about the existence of only one wave. Thus, Figs. 4, *a* and *b* demonstrate how the dispersion  $n(\omega)$  calculated by KKR's differs from that measured experimentally in the case where SD  $\varepsilon(\omega, \mathbf{k})$  is considerable.

**B.** Experimentally measured values of  $n(\omega)$  and  $\kappa(\omega)$  can be used to calculate the real and imaginary parts of the dielectric permittivity function. The dependences obtained are shown in Fig. 4, *c* by solid curves 1 and 2, respectively. While carrying out calculations according to formulas (21) and (22) for every frequency  $\omega$ , only one of the measured  $n(\omega)$ -values was taken, namely, which corresponded to a wave with higher intensity. Therefore, starting from the longitudinal frequency  $\omega_L$ , the values of the refractive index for the “+”-wave were discarded.

For the sake of comparison between the experiment and the theory, relations (8) and (9) were rewritten in the forms valid for positive  $\omega$ 's [19]:

$$\varepsilon'(\omega) = 1 + \frac{2}{\pi} \int_0^{\infty} \frac{x\varepsilon''(x)}{x^2 - \omega^2} dx, \quad (23)$$

$$\varepsilon''(\omega) = -\frac{2\omega}{\pi} \int_0^{\infty} \frac{\varepsilon'(x)}{x^2 - \omega^2} dx. \quad (24)$$

Relation (23) can be used to calculate the dependence  $\varepsilon'(\omega)$  on the basis of the known dependence  $\varepsilon''(\omega)$ ; and vice versa: relation (24) can be used to calculate the dependence  $\varepsilon''(\omega)$  on the basis of the known dependence  $\varepsilon'(\omega)$ . The corresponding results of calculations are depicted in Fig. 4, *c* by dashed curves 3 and 4, respectively. Their cardinal difference from the initial dependences – curves 1 and 2 – is evident, which testifies that the use of relations (23) and (24) is incorrect in cases where SD  $\varepsilon(\omega, \mathbf{k})$  is substantial [47].

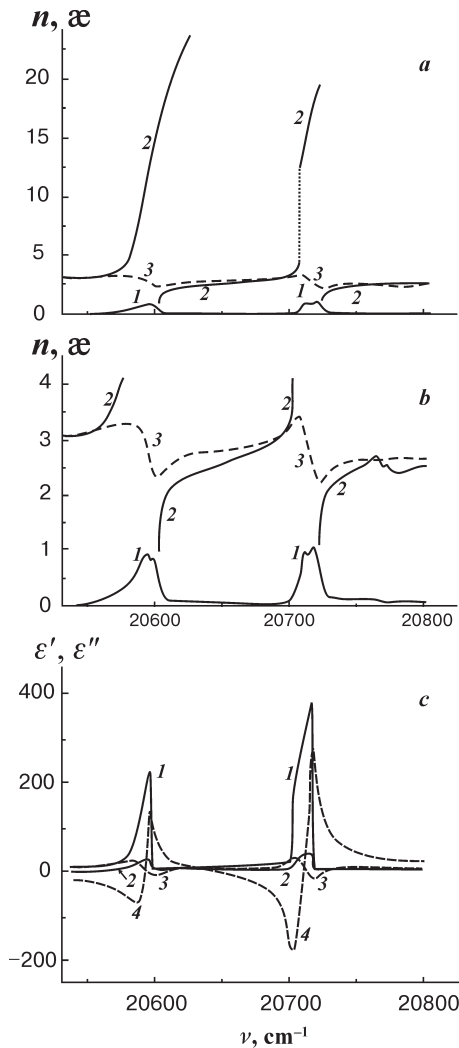


Fig. 4. *a* and *b* – dispersion  $n(\omega)$  measured experimentally (2) and calculated theoretically (3) by relation (21) on the basis of the absorption spectrum  $\kappa(\omega)$  (1). *c* – dependences  $\epsilon'(\omega)$  and  $\epsilon''(\omega)$  (curves 1 and 2), derived from experimentally measured dependences  $n(\omega)$  and  $\kappa(\omega)$ , and the dependences conjugated to them (i.e. calculated by relations (23) and (24) (curves 3 and 4) [47]

### 4.2. Invalidity of Fresnel formulas

#### 4.2.1. Spectral dependence of the reflection coefficient

In work [43], it was shown for the first time that if the  $\kappa(\omega)$ - and  $n(\omega)$ -dependences experimentally measured in works [36, 37] should be substituted into the Fresnel formula (6), the calculated spectrum of reflection from a semiinfinite medium  $R(\omega)$  would drastically differ from the experimentally measured one. In particular,

the calculated dependence  $R(\omega)$  would increase with the frequency  $\omega$  owing to the growth of  $n(\omega)$  within the absorption band halfwidth, whereas the experimental one revealed an anomalous section there (Fig. 5,a). This contradiction of the single-wave theory was overcome in work [48], where the experimental data were demonstrated to be in good agreement with the results of theoretical calculations in the framework of Pekar’s theory.

First, three points from experimentally measured  $\kappa(\omega)$ - and  $n(\omega)$ -curves were used to determine the parameters of the theory  $\epsilon_0$ ,  $A$ ,  $\omega_0$ , and  $\Gamma$ , which are needed for carrying out further calculations. Then, the dependences  $\kappa(\omega)$  and  $n(\omega)$  for the “+”- and “-”-waves were calculated and agreed well with experimental ones. Moreover, it turned out that the “+”-wave was transmitted through the crystal only at frequencies below the frequency of a longitudinal exciton  $\omega_L$ , and the “-”-wave only at frequencies above  $\omega_L$  (similarly to solid curves in Fig. 1,c).

According to Pekar’s theory, the expression for the reflection coefficient  $R(\omega)$  in the case of a semiinfinite crystal looks like [1, 36]

$$R = \left| \frac{\tilde{n}_+ - 1 - q(\tilde{n}_- - 1)}{\tilde{n}_+ + 1 - q(\tilde{n}_- + 1)} \right|^2, \tag{25}$$

where

$$q = |q|e^{i\Phi} \equiv \frac{\epsilon_0 - \tilde{n}_+^2}{\epsilon_0 - \tilde{n}_-^2} = -\frac{E_-}{E_+},$$

$E_+$  and  $E_-$  are the complex amplitudes of the “+”- and “-”-waves, respectively, which emerge in the crystal. In work [9], it was shown that the expression for  $R(\omega)$  can be rewritten in the form of the usual Fresnel formula (6), where the refractive index  $\tilde{n}(\omega) = n(\omega) + i\kappa(\omega)$  of the single-wave theory must be substituted by an “effective” one,  $\tilde{n}_{\text{eff}} = n_{\text{eff}} + i\kappa_{\text{eff}}$ , which is a complicated function of  $\tilde{n}_+$  and  $\tilde{n}_-$ :

$$R = \left| \frac{\tilde{n}_{\text{eff}} - 1}{\tilde{n}_{\text{eff}} + 1} \right|^2, \quad \tilde{n}_{\text{eff}} = \frac{\epsilon_0 + \tilde{n}_+\tilde{n}_-}{\tilde{n}_+ + \tilde{n}_-} \equiv \frac{\tilde{n}_+}{1 - q} + \frac{\tilde{n}_-}{1 - 1/q}. \tag{26}$$

Therefore, the higher the amplitude of either wave, the larger its contribution to  $\tilde{n}_{\text{eff}}$ . Hence, the manifestation of the “+”- and “-”-waves in reflected light is reduced to the formation of an “effective” value for the refractive index in formula (26). The corresponding dependences  $n_{\text{eff}}(\omega)$  and  $\kappa_{\text{eff}}(\omega)$  are depicted in Fig. 1,c. They are similar to the relevant curves of a classical oscillator

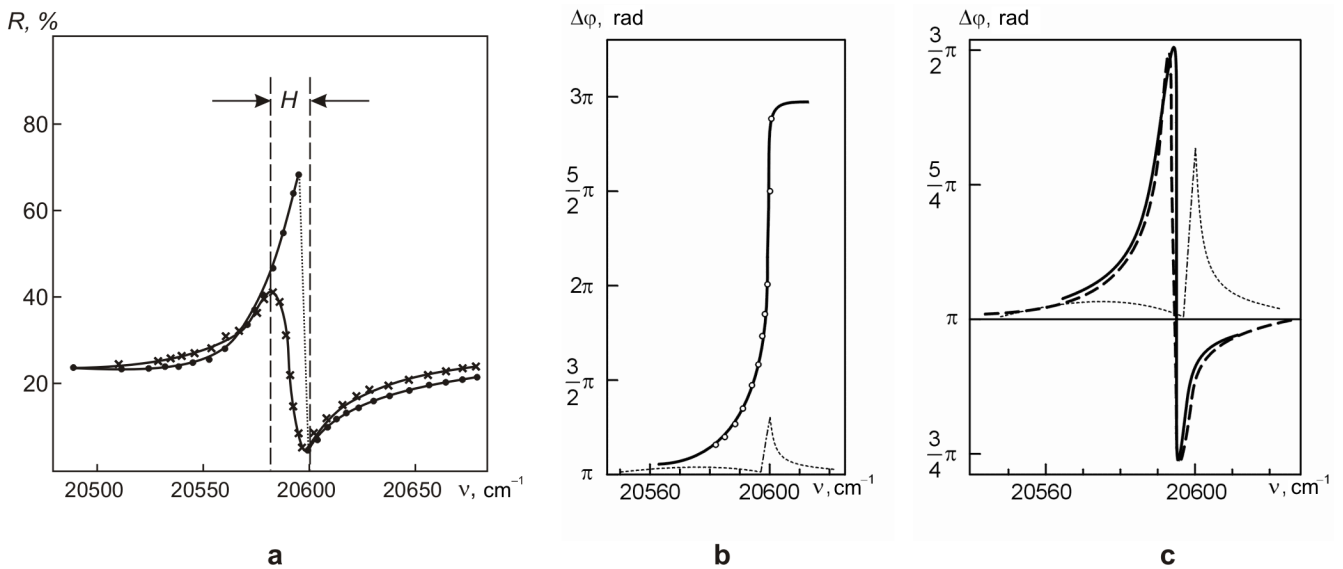


Fig. 5. Spectral dependences of the intensity (a) and the phase (b, c) of the reflected wave in the range of  $A_{n=1}$ -exciton in the CdS crystal,  $\mathbf{E} \perp \mathbf{C}$ ,  $T = 4.2$  K. Crosses in panel a correspond to values experimentally measured in work [43], circles in panel b to experimental values of work [49], and the dashed curve in panel c to experimental values of work [50]. The results of calculations in the framework of single-wave theory: a – solid circles; b, c – dotted curves. The results of calculations in the framework of the ALW theory with a dead layer on the crystal surface are plotted by solid curves ( $\Gamma = 0$  and  $d = 8$  nm (b);  $\Gamma = 1.37$  cm $^{-1}$  and  $d = 8.35$  nm (c))

(Fig. 2,b) and are responsible for the formation of a classical profile of the reflection spectrum with anomalous section (Fig. 1,d), which agrees well with experimentally measured one [48] (see Fig. 5,a).

#### 4.2.2. Spectral dependence of the phase variation of a reflected wave

On the basis of the measured dependences  $n(\omega)$  and  $\kappa(\omega)$  and using the Fresnel formula (7), one can also calculate the phase variation  $\Delta\varphi(\omega)$  at light reflection (the dotted curves in Figs. 5,b and c). The experimental dependences  $\Delta\varphi(\omega)$  measured for “thick” CdS crystals are shown in Fig. 5,b by circles and in Fig. 5,c by a dashed curve. It is evident that they are quite different from the dependence calculated by formula (7) of the single-wave theory.

If one takes advantage of the effective refractive index, which makes allowance for both Pekar waves (the solid curves in Fig. 5,b and c), a very good agreement with experimental data is attained. In this case, one is forced to apply Pekar’s ABCs at some distance from the crystal surface, i.e. to introduce a dispersionless “dead” layer (DL) with the thickness  $d$  equal to two to three times  $r_{\text{ex}}$ , which excitons cannot penetrate into, not being destroyed, and where  $\varepsilon = \varepsilon_0$ . The concept of ABC was introduced by Hopfield in work [9]. Note that the introduction of a DL while calculating  $\Delta\varphi(\omega)$  in the

framework of the single-wave theory, i.e. while using the measured values of  $n(\omega)$  and  $\kappa(\omega)$ , does not give rise to agreement with experiment.

Different kinds of curves in Figs. 5,b and c correspond to different values of the parameter  $\Gamma$ , which evidences for different degrees of perfection of crystals in specimens that were used for measurements. Later on, similar  $\Delta\varphi(\omega)$  spectra were obtained in work [51], where the transformation of curves from type (b) to type (c) occurred under temperature elevation, i.e. under growing  $\Gamma$ . Figure 6 illustrates the ranges of a possible variation of the exciton transition parameters – the DL thickness  $d$  and the damping constant  $\Gamma$ , – for which the phase curves and the reflection spectra turn out of different types [50].

Thus, in order to put the theoretical spectra of reflection and phase variation at reflection in agreement with the experimental ones, the additional wave has to be taken into consideration, i.e. the effective refractive index has to be used in calculations.

#### 4.3. Dependence of the refractive index on the crystal thickness

In the works cited above, it was reliably established that only the “+”-wave can be transmitted through a CdS

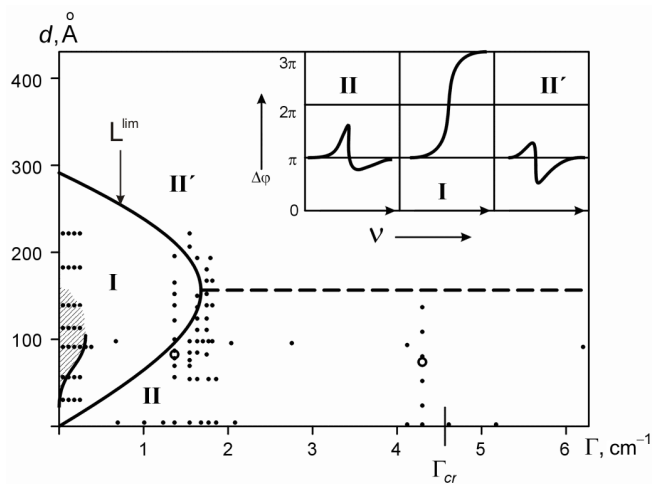


Fig. 6. Ranges of the parameters  $\Gamma$  and  $d$  which correspond to the  $\Delta\varphi(\omega)$ -solutions of different types. Points correspond to  $\Gamma$  and  $d$  values, which were used for calculating  $\Delta\varphi(\omega)$  and  $R(\omega)$ . Circles are drawn around those points, for which the agreement between the calculated and experimental curves at  $T = 4.2$  and  $77$  K was the best. Curves  $\Delta\varphi(\omega)$  typical of every parameter range are depicted in the inset. In the hatched region, the  $R(\omega)$ -curves have a spike structure [50]

crystal at low temperatures and in the frequency range below  $\omega_L$  of  $A_{n=1}$ -exciton. Therefore, Fabry–Perot formula (18) seemed reasonable to be applied for measuring the dependence  $n(\omega)$  for transmitted light. In works [52, 53], where formula (18) was used, the dispersion curve  $n(\omega)$  in the resonance region was found to be shifted towards short waves, as the crystal thickness diminished. The authors of work [52] associated this displacement with the variation of the resonance frequency  $\omega_0 \equiv \omega_T$ . In work [53], it was demonstrated that the shift of the dispersion curve is not accompanied by the variation of the longitudinal frequency  $\omega_L$  position; the latter remains constant, which means that it is  $\Delta_{LT}$  that changes. In Figs. 7, *a* and *b*, the experimental data taken from those works are exhibited.

Recent calculations [54] demonstrated that the effect observed was caused by an ineligible application of the single-wave-theory formula to a situation where the presence of an additional wave was substantial. According to Pekar’s theory, the expressions for the transmission,  $T$ , and reflection,  $R$ , coefficients of a crystalline plate with finite thickness look like [12]

$$T = \frac{4|G|^2}{|(1 + iF)^2 + G^2|^2}, \tag{27}$$

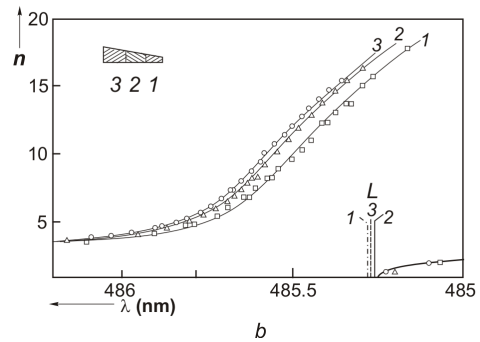
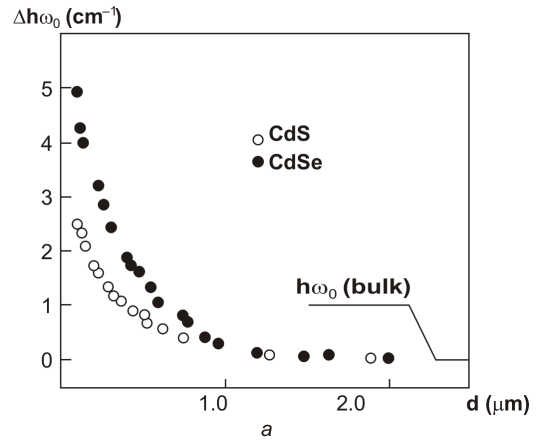


Fig. 7. *a* – Dependences of the resonance frequency  $\omega_0$  shift for  $A_{n=1}$ -excitons in CdS and CdSe crystals on their thickness  $d$ ;  $T = 1.6$  K (according to data of work [52]); *b* – Experimental (points) and theoretical (solid curves) dispersion curves for CdS crystals with various thicknesses  $d = 0.18$  (1),  $0.27$  (2), and  $0.36 \mu\text{m}$  (3).  $L$  denotes the corresponding position of the longitudinal exciton energy.  $T = 4.2$  K,  $\mathbf{E} \perp \mathbf{C}$  (according to data of work [53])

$$R = \frac{|1 + F^2 - G^2|^2}{|(1 + iF)^2 + G^2|^2}, \tag{28}$$

where

$$F = \frac{\tilde{n}_+}{(1 - q)} \text{ctg}(k_+d) + \frac{\tilde{n}_-}{1 - 1/q} \text{ctg}(k_-d),$$

$$G = \frac{\tilde{n}_+}{(1 - q) \sin(k_+d)} + \frac{\tilde{n}_-}{(1 - 1/q) \sin(k_-d)},$$

$$k_{\pm} = \frac{\omega}{c} \tilde{n}_{\pm}.$$

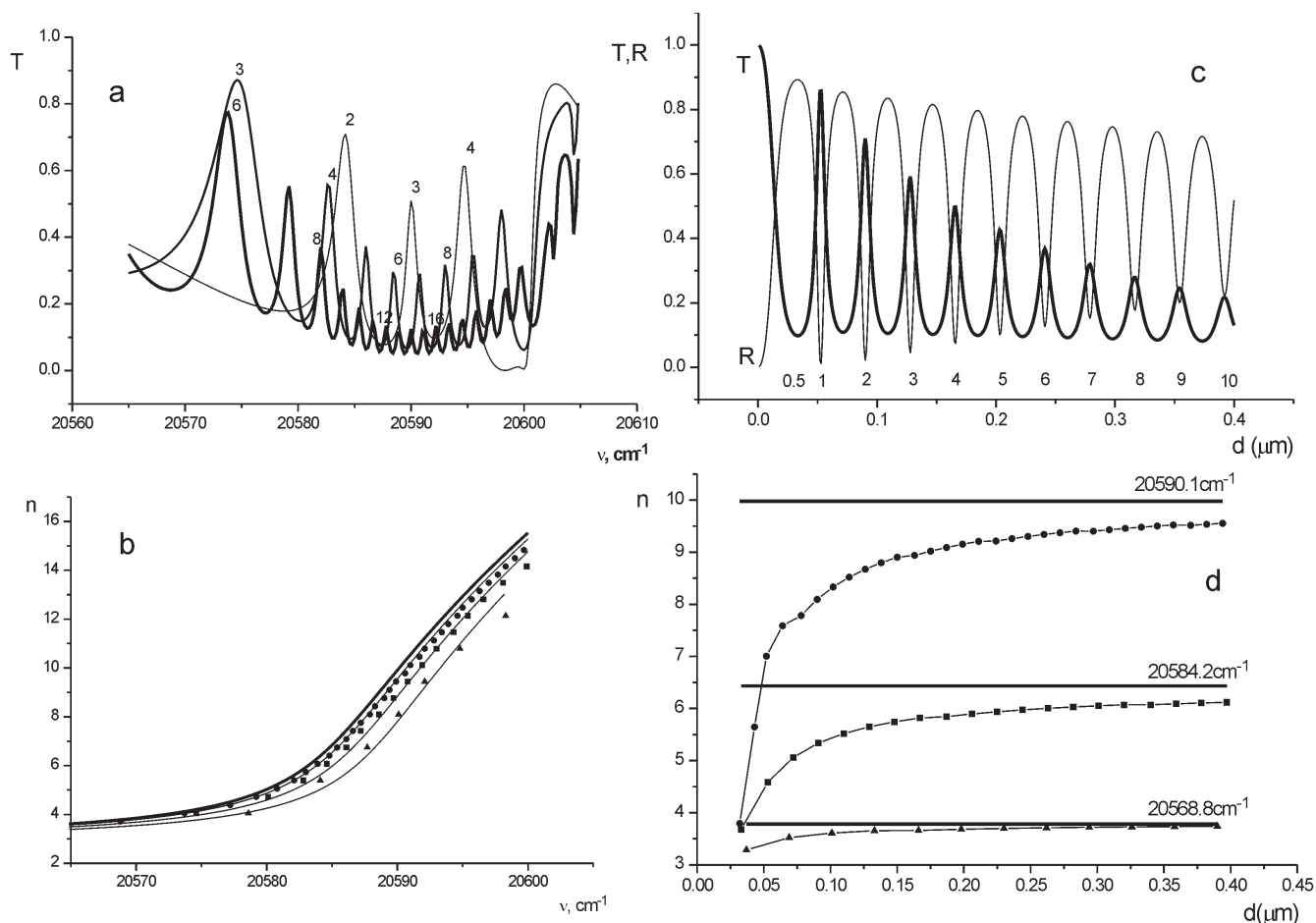


Fig. 8. *a* – Transmittance spectra for three CdS crystals, calculated in the framework of Pekar’s theory; the thicknesses of the crystal plates are (in  $\mu\text{m}$  units) 0.09 (thin curve), 0.18 (medium curve), and 0.36 (thick curve). Numbers near maxima correspond to interference orders. *b* – Results of calculations of dispersion curves  $n(\omega)$  from interference extrema (panel *a*) by the Fabry–Perot formula:  $d = 0.36$  (points), 0.18 (squares), and 0.09  $\mu\text{m}$  (triangles); the thick curve corresponds to the  $n_+(\omega)$ -dependence, the thin curves are the approximations of shifted curves under the reduction of  $\Delta_{LT}$ ; similar curves are obtained under shifting  $\omega_0$  as well. *c* – Dependences of crystal transparency  $T$  (thick curve) and reflection  $R$  (thin curve) on the crystal thickness, calculated in the framework of Pekar’s theory for  $\omega = 20584.2 \text{ cm}^{-1}$ . The numbers correspond to interference orders. *d* – Dependences of the “effective” refractive index for transmitted light on the crystal thickness for various frequencies from the exciton resonance range of the spectrum. Solid lines parallel to the horizontal axis denote the values of  $n_+$  for the same frequencies [54]

In Fig. 8,*a*, three theoretical transmission spectra for CdS crystal plates with the thickness ratios 1:2:4, calculated by formula (27), are depicted. It is evident that, in contrast to relation (18), their multiple interference orders do not coincide with one another by frequency. But if formula (18) is applied to every spectrum and the corresponding dispersion curves of the refractive index are taken into account, as was done in works [52, 53], the spectra prove to be shifted towards a short-wave side – the thicker the specimen, the larger the displacement, – just as was registered

in experiment (Fig. 8,*b*). It should be emphasized that, while calculating the transmission spectra, the theoretical parameters for all three curves were constant, i.e. neither  $\omega_0$  nor  $\Delta_{LT}$  was varied.

One can use formulas (27) and (28) to calculate the dependences of the transmission and reflection coefficients on the crystal thickness (Fig. 8,*c*). Then, it happens that the interference extrema are not spaced equidistantly from one another. It turns out that the thinner is the crystal, the larger is the period of oscillations; i.e. in order that the following interference

extremum may be formed, light has to cover a longer distance in a thin crystal than it does in a thick one. The plotted dependences  $T(\omega)$  for three  $\omega$ -values from the  $\Delta_{LT}$  range, being treated by the classical formula (18), give rise to curves presented in Fig. 8, *d*. The latter clearly illustrate the dependence of the “effective” refractive index for the transmitted wave on the crystal thickness. It is obvious that the effect in the considered interval of thicknesses was obtained owing to the application of formulas of the single-wave theory to the situation where SD is essential.

Moreover, the “effective” absorption coefficient for the transmitted wave also depends on the specimen thickness. The failure of the Bouguer–Lambert law was unequivocally demonstrated in experiments carried out with a paradichlorobenzene crystal in the range of the pure electron transition resonance frequency and at  $T = 4.2$  K. The dependence to the logarithm of transparency on the crystal thickness has a characteristic cusp, which separates two linear sections, with the slope of each of them being determined by different, by value, absorption coefficients. The description of this phenomenon and its theoretical consideration is expounded in work [14] in detail.

### 5. Temperature Dependence of Spatial Dispersion Effects and Transition to Classical Crystal Optics

As the temperature of the crystal grows, the exciton-phonon interaction becomes stronger and, as a consequence, the constant  $\Gamma$ , inverse to the exciton lifetime, becomes larger. Therefore, in order to predict the temperature dependence of the SD effects theoretically, one has to trace the variations of crystal optical characteristics with growing  $\Gamma$ . For the first time, it was done for an anthracene crystal in work [56]; it was shown that there exists the so-called critical temperature  $T_{cr}$ , which corresponds to a certain critical value of the constant  $\Gamma_{cr}$  and above which the optical properties of the medium with the SD can be described by the formulas of classical crystal optics. In work [57], analogous calculations were executed for a CdS crystal.

As was already emphasized above, according to Pekar’s theory, there is no energy absorption in the crystal if  $\Gamma = 0$ . In this case, the transmission and reflection coefficients of a plate with finite thickness obey the relation  $T + R = 1$ . At interference transmission maxima,  $T = 1$  and  $R = 0$ ; at corresponding minima,  $T = 0$  and  $R = 1$  [12].

If  $\Gamma \neq 0$ , there appears the true energy absorption in the crystal, and the refractive indices of both waves become complex: the “+”-wave acquires a  $\kappa_+$ -branch, and the  $n_-$ - and  $\kappa_-$ -branches of the “-”-wave become prolonged to the both sides from the frequency  $\omega_L$ . In this case, the  $\kappa_+$ -branch, which has an asymmetric bell-shaped profile, sharply rises as the parameter  $\Gamma$  grows, which – from the theoretical viewpoint – should give rise to a strong enhancement of absorption, while the crystal is heated up. In the  $n_-$ -branch, near the frequency  $\omega_T \equiv \omega_0$ , there emerges a characteristic maximum, the amplitude of which drastically increases as  $\Gamma$  grows. At the *critical value*  $\Gamma_{cr}$ , this maximum reaches the  $n_+$ -branch, and the refractive indices of both waves become identical. If the parameter  $\Gamma$  grows further, each branch has a discontinuity point at this frequency, with the corresponding continuations being different; therefore, each curve is a combined one: the  $n_+$ - and  $\kappa_+$ -branches transform into the  $n_-$ - and  $\kappa_-$ -ones, respectively, and vice versa, the  $n_-$ - and  $\kappa_-$ -branches transform into the  $n_+$ - and  $\kappa_+$ -ones, respectively. The “plus-to-minus” curves have ordinary classical profile (in particular, this concerns a dispersion  $n(\omega)$ -curve with anomalous section), while the “minus-to-plus” ones demonstrate a nonclassical behavior (see Figs. 9, *a* and *b* below). In the case of a semiinfinite crystal, the spectrum of the reflection coefficient  $R(\omega)$  has an ordinary classical shape with anomalous section at all  $\Gamma$ -values, as if a single wave with  $n_{eff}$  and  $\kappa_{eff}$  propagates in the crystal.

Thus, it follows from the consideration above that the area under the absorption curve should drastically increase, as the parameter  $\Gamma$  varies from 0 to  $\Gamma_{cr}$  (mainly owing to the growth of the parameter  $\kappa_+$ ), and then it should remain constant, because the broadening of the absorption curve is compensated by a reduction of its maximum. The profiles of dispersion curves should undergo a characteristic transformation, from a curve with discontinuity at the frequency  $\omega_L$  to a curve with anomalous section. These theoretical predictions were confirmed experimentally.

#### 5.1. Absorption

In work [58], it was found that, if the temperature is increased from 1.8 to 180 K, the area under the absorption curve of  $A_{n=1}$ -exciton in a CdS crystal 0.3  $\mu\text{m}$  in thickness sharply grows first, approximately by an order of magnitude, and then, above 77 K, becomes stabilized. The authors of work [59] successfully explained this effect in the framework of Pekar’s theory and, hence, obtained a very important experimental

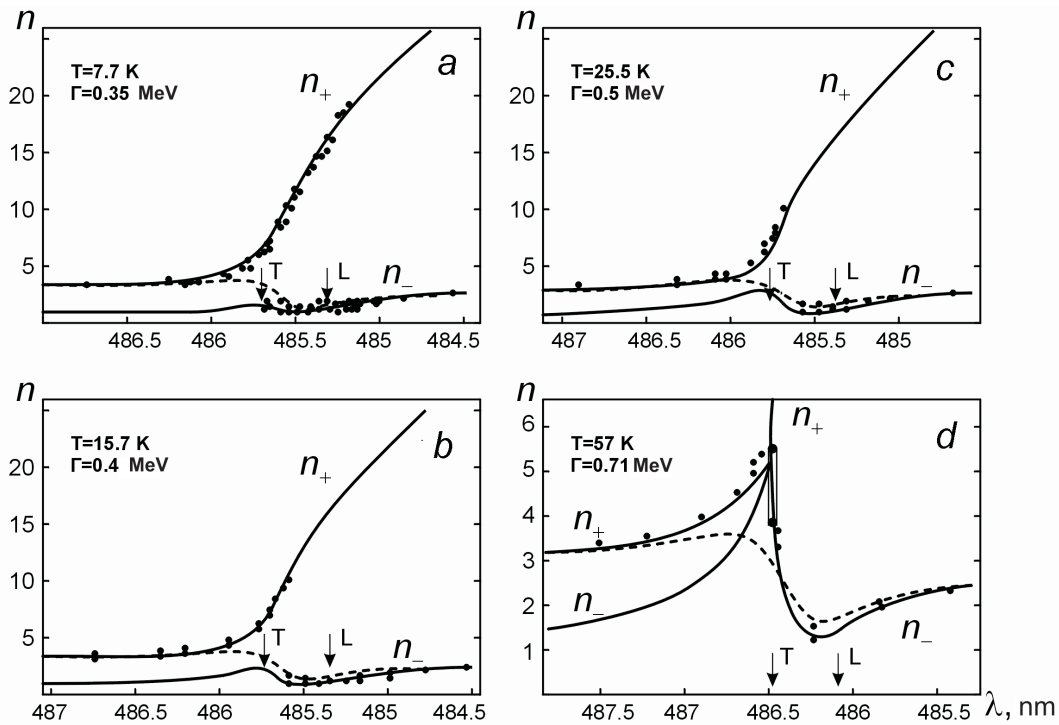


Fig. 9. Dispersion of the refractive index in the range of  $A_{n=1}$ -exciton at various temperatures. Points correspond to the experimental data, solid curves to the theoretically calculated  $n_+(\omega)$ - and  $n_-(\omega)$ -dependences, dashed curves to the  $n_{\text{eff}}(\omega)$ -dependence [17]

proof of its prediction ability. At the same time, the area under the curve of the pure electron absorption band in paradichlorobenzene crystals was shown in work [55] to become almost 6 times larger, when the temperature grew from 1.8 to 100 K. In Davydov's book [14], these experiments were described in detail, and the analytical expressions concerning the dependences of the integrated absorption coefficient, halfwidth, and maximum of the exciton band on the damping constant of an exciton were presented.

In works [60–63], this direction of researches has obtained a new impetus. In work [60], Akhmediev derived a simplified relation which describes the dependence of the integrated coefficient of exciton absorption (IEAC) on the damping constant. According to the results of work [60], the IEAC linearly depends on  $\Gamma$  at small  $\Gamma$ 's and tends to zero at  $\Gamma \rightarrow 0$ . Starting from  $\Gamma_{\text{cr}}$ , the IEAC becomes stabilized. In works [61–63], the effect concerned was studied experimentally in the range of  $A_{n=1}$ -exciton of CdS and CdSe crystals. In all cases, the temperature growth was accompanied by a substantial increase of the IEAC. In work [63], measurements were carried out in the mixed photon-like-exciton mode, at various angles of light incidence onto the crystal surface, and in the temperature interval

4.2–120 K. According to the theory, the larger is the angle of light incidence, the larger is the longitudinal-transverse splitting in the mixed mode, and the higher is the critical temperature, starting from which the IEAC becomes stabilized.

## 5.2. Dispersion of the refractive index

The transition to classical crystal optics, which is induced by the transformation of dispersion curves, was first traced experimentally by monitoring the interference pattern of polarized beams in a superthin plane-parallel CdS crystal in the course of heating the latter up [64]. Afterwards, the temperature-induced variation of the “+”- and “-”-wave dispersion was studied in detail in work [17], where the method of light refraction by a wedge-shaped CdS crystal was used. This method of registration allowed the characteristic features emerging in the course of reconstruction of dispersion curves to be observed (see Fig. 9). The points in the figure are the experimental data, and the solid curves are the dependences  $n(\lambda)$  calculated in the framework of Pekar's theory for various  $\Gamma$ -values. For the plots to be most illustrative, the temperatures, at which the most typical features

of spectrum reconstruction manifest themselves, were chosen.

We would like to emphasize two most characteristic issues. As a temperature  $T = 7.7$  K is achieved (cf. the case  $T = 1.8$  K, Fig. 3,*b*), the whole  $\Delta_{LT}$  range becomes suddenly “translucent” for the “-”-wave, so that the spectral interval of coexistence of two transmitted light waves becomes substantially broadened (see Fig. 9,*a*), and the “-”-wave starts to manifest itself explicitly. This occurs when the parameter  $n_-$ , in the course of  $\Gamma$  growing, reaches a unity value, and the “-”-wave changes its status from the reflected by the crystal to that which can propagate inside. On the other hand, the fact that this phenomenon has a threshold character testifies that the amplitude of the “-”-wave is large in the whole  $\Delta_{LT}$  range.

At the further elevation of the temperature, besides the variation of the  $n_{\pm}(\lambda)$ -curves behavior, the growth of absorption becomes of great importance. The “+”-wave range becomes more and more truncated from its high-energy side (Figs. 9,*b* and *c*), so that the range of wave overlapping becomes substantially narrowed at  $T = 15.7$  K and practically disappears at  $T = 25.5$  K. The absence of the anomalous dispersion section and the jump of experimentally measured values from the  $n_+$ -branch onto the  $n_-$ -one remain to be the characteristic features of the curves. The jump point is located within the  $\Delta_{LT}$  interval and gradually approaches the frequency  $\omega_T$ .

At last, at a temperature that corresponds to the critical value  $\Gamma_{cr}$ , the branches of the measured dispersion curve merge together (Fig. 9,*d*). Before the frequency  $\omega_T$ , experimental points fit the “+”-wave branch; after  $\omega_T$ , they permanently transit to the “-”-wave branch, thus forming a single dispersion curve with anomalous section. A characteristic feature of this curve is that its dip occupies an extremely narrow spectral interval. In this case, the laser beam in the focal plane of a measuring microscope transforms from a round light spot into a light strip in the experiment, which corresponds to rather a wide variation of the refractive index from 5.5 to 3.5 (the double line in Fig. 9,*d*). Notwithstanding the presence of the anomalous section, the measured dispersion curve is still appreciably different by shape from the calculated profile of the effective refractive index, which should be used for the approximation of the reflection spectrum (the dashed curve).

An interesting method of transition to classical crystal optics has been demonstrated in work [65], where the refractive index dispersion was measured for a

wedge-shaped CdS crystal in the mixed mode and at  $T = 1.8$  K. By varying the angle of light incidence, the authors changed the effective values of  $\Delta_{LT}$  and, hence, of  $\Gamma_{cr}$ . They consistently traced the variation of the  $n(\omega)$ -curves until the dispersion curves manifested anomalous sections, but the overlapping of “+”- and “-”-waves was not observed owing to a relatively large thickness of specimens.

Note that, in different specimens, the value  $\Gamma_{cr}$  can be attained at different temperatures, which is associated with the degree of crystal perfection, the presence of impurities and defects, the deformation state, and so on. For instance,  $T_{cr} \approx 60$  K in “free” perfect CdS crystals, and  $T_{cr} \approx 20$  K in specimens which are in optical contact with the substrate. In this case, the simplest, but rough enough, criterion for the determination of  $T_{cr}$  of a specific crystal could be a temperature, at which the width of its absorption band – or the corresponding width of the reflection spectrum – starts to grow at specimen heating. This suggestion was confirmed by calculations carried out in work [62] taking SD into account in the framework of Pekar’s theory, as well as experiments which were analyzed in detail in work [66].

It is of interest to confront the parameters of exciton transitions and, correspondingly, the values of  $\Gamma_{cr}$  and  $T_{cr}$  in some substances (see Table). As one can see, the variation ranges of the parameters are very large; therefore, the ALW manifestations can be different. In an anthracene crystal, for instance, the effective mass and  $\Delta_{LT}$  are very large, and the asymptote deviates insignificantly from a vertical line; therefore, an additional wave arises near the resonance frequency without going beyond the  $\Delta_{LT}$  limits. This crystal exhibits very strong polariton effects, but ALWs are not actual already at  $T > 15$  K. Light, which propagates in the crystal, is described by a single normal wave, and the corresponding value of the refractive index slightly differs from those calculated without taking SD into account [14]. In the case of the simplest amorphous xenon cryocrystal with the intermediate type of coupling between atoms, the value of  $\Delta_{LT}$  is large, while the value of  $M$  is relatively small. The whole temperature interval, where the solid phase exists, is located below  $T_{cr}$ , which

Substance	$\Delta_{LT}$ , $\text{cm}^{-1}$	$M$	$\Gamma_{cr}$ , $\text{cm}^{-1}$	$T_{cr}$ , K	Reference
Semiconductor CdS	16	$0.8m_e$	5.6	$\sim 60$	[17]
Anthracene molecular crystal	400	$1000m_e$	0.4	$\sim 15$	[14]
Xenon cryocrystal	800	$2.2m_e$	$\sim 88$	$> 100$	[15]

is favorable for the observation of the additional-wave and polariton effects [15].

## 6. Influence of the Surface on the Reflection Spectra of Crystals and the Features of Their Approximation

The reflected light wave is a carrier of information about the bulk properties of the crystal, on the one hand, and about the state of the crystal surface, on the other hand. Therefore, the determination of such theoretical parameters, which would make the description of the bulk and the surface of the crystal possible using the measured characteristics of only the reflected wave, is a difficult task, and, in some cases – e.g., provided that the SD effect is important – ambiguous.

### 6.1. ABCs and theoretical models of surface influence

From the viewpoint of theoretical consideration of even a perfect crystal, the presence of SD gives rise to the necessity of introducing ABCs, which depend substantially on the type of the exciton state under consideration. Pekar's ABC (5) has been derived for a Fresnel exciton with small radius. For a Wannier–Mott exciton with large radius  $r_{\text{ex}}$ , Hopfield, as was indicated above, has introduced a dispersion-free “dead” layer on the crystal surface (7).

Later on, the issue of ABCs was examined in tens of theoretical works; nevertheless, the discussion about the correctness of these or those ABCs, as well as about a possibility to obtain the solution of the problem in general, without introducing ABCs, is still being continued. The problem has been analyzed in detail in works [10, 12, 14] and in the work by Ivchenko in collective monograph [11]. Pekar repeatedly emphasized that “ABCs cannot be postulated, adopted without any proof, or introduced as a working hypothesis which is to be checked experimentally. While considering a system of charged particles that interact with an electromagnetic field, the latter is determined by the Maxwell equations, and the state of particles by the temporal Schrödinger equation. Therefore, ... every boundary condition in the problem concerned – in particular, ABC – has to follow from the Schrödinger equation and the Maxwell ones” [12]. Pekar showed that “knowing the laws of exciton reflection is not only necessary, but also sufficient for the derivation of a necessary number of ABCs and the unambiguous solution of the problem dealing with the reflection and

transmission of light waves through a vacuum–crystal interface”. He has derived ABC (5) under conditions that the exciton wave is reflected from the crystal surface.

In some works (see, e.g., work [67]), it is the derivative of polarization at the crystal boundary that is supposed zero:

$$(dP_{\text{ex}}/dz)_{z=0} = 0. \quad (29)$$

In this case, the exciton wave function has an antinode at the surface rather than a node, as was for Pekar's ABC. In works [68–71], specific models were used to demonstrate that the general form of the ABC is

$$\left[ \alpha(\omega)P_{\text{ex}} + \beta(\omega) \frac{dP_{\text{ex}}}{dz} \right]_{z=0} = 0. \quad (30)$$

The same relation was derived in work [10], proceeding from general phenomenological ideas concerning the polarizability kernel in Eq. (1).

Concerning the works, where ABCs for a finite crystal were asserted to be of no use at all, Pekar in work [72] wrote: “... if photon-like exciton solutions are deduced as linear combinations of solutions obtained for an infinite crystal, the ABC are necessary. But if the polarization response of a semiinfinite crystal is known, ... no ABCs are needed any more”.

In a number of works (see, e.g., works [73, 74]), “a dielectric approximation” is applied while solving the problem without using ABCs. In works [10, 12], this approximation was shown to be incorrect, because it contradicts the conservation law of energy. In his work [75] and book [14], Davydov, without introducing ABCs, used the method of extraneous currents on the crystal surface. The following expression was obtained for a constant  $q$  which determines the ratio between the amplitudes of normal waves,

$$q = \frac{(\varepsilon_0 - \tilde{n}_+^2)\tilde{n}_+}{(\varepsilon_0 - \tilde{n}_-^2)\tilde{n}_-}, \quad (31)$$

and which differs from Pekar's one (25) by an extra multiplier. The same ratio between the amplitudes of transmitted waves can be derived from ABC (29).

Recently, work [76] which invoked a fierce discussion [77–80] had been published. Its author asserted that the introduction of additional boundary conditions by Pekar for the solution of problems in crystal optics, provided that there are additional light waves, was “a historical mistake”, and one can do without using ABCs at all. But the results of works [77, 80] have demonstrated that the author of work [76] had obtained a well-known result,

which is similar to that obtained by Davydov in work [14]; therefore, this result also corresponds to ABC (29).

It should be noted that the surface of real crystals can be distorted owing to various defects of growth, a high concentration of adsorbed atoms, and so on. If defects and adatoms are charged, the surface gets a total electric charge, which, together with the electrostatic image forces, affects the surface-induced band bending, and, therefore, the variation of the surface potential of excitons, which can give rise to the modification of the reflection spectrum profile in comparison with that for a perfect crystal.

The most fruitful for the explanation of characteristic features in the reflection spectra of real crystals are the theories by Sugakov [68–70], Davydov and Myasnikov [81], and Kiselev [82]. Those theories consider an opportunity for a non-intrinsic surface layer caused by the difference between near-surface and bulk properties of real crystal – in particular, the dependences  $\omega_0(z)$  and  $\Gamma(z)$  – to be created. In Kiselev’s theory [82], SD was taken into account both in the bulk and the transition layer of a crystal. Various versions of the potential, which could be expected to occur in real crystals, have been examined: a potential drop into the depth, a rigid wall near the surface, and a potential well near the surface. The reflection spectra have been shown sensitive to the surface state, i.e. such phenomena as the emergence of spikes, contour inversion, and the appearance of an extra structure have been explained. The author of work [82] specially emphasized: “The inverse problem – the restoration of the potential profile from scattering data, i.e. from the shape of a reflection contour – has no unambiguous solution”.

## 6.2. Comparison with experiment

Since work [9] was published, a lot of other authors have demonstrated that, for many semiconductor crystals, the reflection spectra of high-quality specimens measured at low temperatures are well described by Pekar’s theory, which takes the DL on the crystal surface into account. In work [9], the appearance of a spike in the  $R(\omega)$ -curve minimum, which is often observed in the spectra of CdS crystals at low temperatures, was explained for the first time. It arises owing to the interference between light beams that are reflected from the crystal surface and the internal DL boundary. The hatched region in Fig. 6 denotes the narrow range of values for the parameters  $d$  and  $\Gamma$ , at which the calculated spectra contain the spike structure.

The results of calculations carried out in work [83] showed that the increase of the DL thickness  $d$  gives rise to characteristic modifications of the  $R(\omega)$ -curve shape; in particular, these are a reduction of the main maximum height at a frequency of about  $\omega_T$  and the emergence and the further growth of a maximum in the vicinity of  $\omega_T$  up to the “inversion” of the curve shape. As the parameter  $d$  increases further, the curve returns back to its initial form. The complete cycle of the curve shape variation corresponds to the growth of the phase difference between the interfering beams up to  $\theta = 4\pi dn_0/\lambda = 360^\circ$ , when  $2dn_0 = \lambda$  ( $n_0$  is the background refractive index). The experimental results obtained in work [83] became a convincing confirmation of the existence of an intrinsic DL for Wannier–Mott excitons, because there is a correspondence between the DL thickness  $d$  and the exciton radius, in particular, for states  $A_{n=1}$  and  $A_{n=2}$ .

Especially sensitive to the presence of a DL on the crystal surface are phase spectra which, depending on the  $\Gamma$ - and  $d$ -values, have either an  $S$ - or an  $N$ -like shape. In Fig. 6, the corresponding ranges of  $A_{n=1}$ -exciton parameters in a CdS crystal are separated by a solid curve. The DL is also responsible for the emergence of a negative section in the an  $N$ -like curve, which is preserved in the phase spectra at large  $\Gamma$ -values as well. In work [50], on the basis of measuring the  $\Delta\varphi(\omega)$ -dependence at 4.2 and 77 K, practically identical values were deduced for the DL thickness (8.35 and 7.65 nm, respectively); in work [49], the values of 8 nm was obtained, which proves the validity of the theoretical model for the intrinsic DL. The phase and intensity reflection spectra of a  $\beta$ -AgI crystal, which were experimentally measured in work [84] at various angles of incidence, are also described very well by this model.

Of great interest are works, where various theoretical ABCs were used for the simulation of experimental results. In works [51, 85, 86], the phase and angular measurements of the reflection and thermoreflexion spectra were carried out in the range of  $A_{n=1}$ -exciton in a CdS crystal and at various spatial orientations between the axis  $\mathbf{C}$  and the vectors  $\mathbf{E}$  and  $\mathbf{K}$  of the light wave. It turned out that, in *high-quality* semiconductor crystals, where Wannier–Mott excitons with a large radius are excited, *the reflection spectra and the spectra of phase variation at reflection are described well by Pekar’s ABC with an intrinsic DL on the surface*. The other ABCs, in particular, ABC (29) and the dielectric approximation, describe experimental data considerably worse.

In this connection, it is of interest D.F. Nelson's statement in his report at the 9-th International Symposium "Continuum Models and Discrete Systems (CMD9)", which was held in Turkey in 1998: "... We came to a conclusion that Nature virtually uses Pekar's ABCs."

The reflection spectra of real crystals, measured in various works at low temperatures, are very diverse, which is associated to a great extent with the state of crystal surfaces. The available features are not always managed to be described quantitatively by means of Pekar's theory, ABC (5), and Hopfield's DL for a perfect crystal; but they are succeeded to be put in agreement with more realistic models of surface potential, cited above [87–91]. It is significant that *the spike structure of the spectrum can be obtained, provided the availability of a DL and without SD* [47, 92–94].

Very many experimental works were devoted to studying the purposeful influence of various external factors on crystals: preliminary light-striking [95, 96], etching [97], electron bombardment [98, 99], laser irradiation [100], strong electric fields [101–103], and sputtering a metal onto a semiconductor [104]. In monograph [105], those experiments were described and analyzed in detail, and the most probable mechanisms of the non-intrinsic surface layer formation were indicated. It was demonstrated that such a layer could strongly change the reflection spectrum of a real crystal in comparison with that of a "perfect" one, which should be taken into account while analyzing experimental results.

## 7. Applicability Scope of KKR in the Presence of ALW

### 7.1. Dispersion and absorption curves

It was shown above that the dispersion and absorption curves experimentally measured at low temperatures do not obey relations (21) and (22) or (23) and (24) (see Fig. 4). A detailed analysis of the KKR applicability was carried out in work [47]. One should bear in mind that the KKR for the function  $\varepsilon(\omega)$  have been derived on the basis of the principle of causality, provided that the coupling between an electromagnetic wave and the crystal polarization is local. In work [19], the complex function  $\varepsilon(\tilde{\omega}) = \varepsilon' + i\varepsilon''$  was demonstrated to be single-valued and not to tend to infinity in the upper half-plane of the complex variable  $\tilde{\omega} = \omega' + i\omega''$ , i.e. it has no singular points here. It was just for functions of such a type that Kramers and Kronig [106, 107] derived the integral relations between their real and imaginary parts.

(Below, if the whole plane of the complex variable  $\tilde{\omega}$  is not considered, the notation  $\omega$  for the real part  $\omega' \equiv \text{Re } \tilde{\omega}$  is used.)

Provided that SD is substantial and ALWs emerge, there are two  $\varepsilon(\omega)$ -values for every  $\omega$ -value; this situation corresponds to the propagation of two waves through the crystal. In this case, the practical application of integral relations becomes impossible even from a formal point of view, because it is not clear, which of the values of  $\varepsilon'$  and  $\varepsilon''$ , or their combinations, should be substituted into these relations.

A generalization of the KKR to media with SD, provided that the variables  $\omega$  and  $\mathbf{k}$  are independent of each other, was given for the first time by Leontovich [108]. Further, the issue was considered in works by Davydov [109], Mead [110], Ginzburg and Meiman [111], Agranovich and Ginzburg [10]. An important progress in this direction is related to a cycle of works by Solov'ev and co-authors [112–116], where the supplementary dispersion relations were derived.

In work [47], relations (21)–(24) were tested on their applicability to the calculations – in the framework of Pekar's theory – of the dispersion and absorption curves in the range of  $A_{n=1}$ -exciton in a CdS crystal for various values of the damping constant  $\Gamma$ . All other parameters of the theory were chosen to provide the best agreement between the theoretical and experimentally measured [16, 43]  $n(\omega)$ - and  $\kappa(\omega)$ -curves in the range of  $A_{n=1}$ -exciton at  $T = 4.2$  K.

Before the results obtained will be discussed, we note that the function  $\tilde{n}_{\pm}^2$  has a branch point in the plane of the complex variable  $\tilde{\omega} = \omega' + i\omega''$ , and the position of this point can be determined if one puts the expression under the root in Eq. (4) equal zero:

$$\begin{aligned} \omega' &= \omega_0 + \frac{\varepsilon_0}{\alpha}, \\ \omega'' &= 2\sqrt{\frac{\Delta_{LT}\varepsilon_0}{\alpha}} - \Gamma, \end{aligned} \quad (32)$$

where  $\alpha = 2Mc^2/(\hbar\omega_0^2)$ . The analysis of the branch point motion in the complex plane was carried out by V.M. Pisokovoi [117]. If

$$\Gamma = \Gamma_{\text{cr}} = 2\sqrt{\Delta_{LT}\varepsilon_0/\alpha}, \quad (33)$$

we have  $\omega'' = 0$ , and the branch point is on the real axis at the frequency

$$\omega' = \omega_{\text{cr}} = \omega_0 + \varepsilon_0/\alpha. \quad (34)$$

In this case,  $\tilde{n}_{+}(\omega_{\text{cr}}, \Gamma_{\text{cr}}) = \tilde{n}_{-}(\omega_{\text{cr}}, \Gamma_{\text{cr}})$ , and the dispersion curves intersect at real  $\tilde{\omega}$ -values. If  $\Gamma < \Gamma_{\text{cr}}$ ,

the branch point is located in the upper half-plane of complex frequency  $\tilde{\omega}$ , while, at  $\Gamma > \Gamma_{cr}$ , it transits into the lower half-plane. Therefore, if  $\Gamma < \Gamma_{cr}$ , the contour of integration  $C$ , which runs along the real axis and becomes closed at infinity, encircles the singularity point, so that the usual KKR's in form of Eqs. (23) and (24) cannot be applied. If  $\Gamma > \Gamma_{cr}$ , the branch point is located outside the contour of integration, and the KKR's can be valid. But now, they are satisfied by only one of the waves, with the classical asymptote and shape, while the other, for which the value of  $n$  tends to infinity at  $\omega \rightarrow \infty$ , does not satisfy the condition of function finiteness, and KKR's cannot be written down for it.

Let us illustrate this circumstance by the results of calculations. In Figs. 10, *a* and *b*, the solid curves correspond to Pekar's curves  $n(\omega)$  and  $\kappa(\omega)$ , which were calculated for  $\Gamma = 8 \text{ cm}^{-1} > \Gamma_{cr} = 5.64 \text{ cm}^{-1}$ . The dashed curves are the corresponding dependences calculated by relations (21) and (22). Panel *a* exhibits the data for a classical "plus-minus" wave, for which KKR's are satisfied; panel *b* does it for a nonclassical "plus-minus" wave, for which the curves diverge sharply.

As was pointed out in work [109], if two waves of different types and with different dependences  $n(\omega)$  and  $\kappa(\omega)$  can propagate in a medium, "each such wave can be associated with its own  $\varepsilon(\omega)$ -value". Therefore, the curves  $\varepsilon'(\omega)$  and  $\varepsilon''(\omega)$  for each of the waves were also confronted with the relevant dependences calculated in accordance with relations (23) and (24). It turned out that these relations are obeyed for the classical wave and are not for the nonclassical one. It should be emphasized that, in this case, the amplitude of the additional nonclassical wave tends to zero in accordance with ABC (5).

Afterwards, a series of calculations have been carried out for  $\Gamma = 1 \text{ cm}^{-1} < \Gamma_{cr}$ . First, Pekar's curves  $n_{\pm}(\omega)$  and  $\kappa_{\pm}(\omega)$  were calculated; then, KKR's (21) and (22) were applied to them; and the conjugated dependences obtained were compared with the initial ones. Such a comparison was done for the "+", "-", "minus-plus", and "plus-minus"-waves. In addition, the case of a combined wave, for which the jump from the "+"- to the "-"-branch occurs at the frequency  $\omega_L$ , was considered, because, in work [60], a wave of just this type was used to obtain a good approximation for the contour of integrated absorption. It turned out that in none of the cases considered by the authors did the initial and calculated dependences coincide. Figures 10, *c* and *d* illustrate two variants taken from the whole series of calculations. Similar results were also obtained for the dependences  $\varepsilon'(\omega)$  and  $\varepsilon''(\omega)$ .

Thus, KKR's are well satisfied, if the additional wave becomes insignificant, i.e. at  $\Gamma > \Gamma_{cr}$ . But, if  $\Gamma < \Gamma_{cr}$ , the KKR's are not satisfied, neither for each wave separately nor for any of their combinations.

## 7.2. Application of KKR's to reflection spectra

The KKR's are widely used in modern physics to determine optical constants of a substance on the basis of the measured reflection spectrum. It especially concerns semiconductor materials with strong absorption, because direct measurements of their absorption and dispersion,  $n(\omega)$ , spectra are difficult to be carried out (see, e.g., work [118]). The integral dependence between the reflection coefficient  $R(\omega)$  and the phase variation at light wave reflection  $\Delta\varphi(\omega)$  is determined by the relations [44]

$$\Delta\varphi(\omega) = -\frac{2\omega}{\pi} \int_0^{\infty} \frac{\ln \sqrt{R(x)}}{x^2 - \omega^2} dx, \quad (35)$$

$$\ln \sqrt{R(\omega)} = 1 + \frac{2}{\pi} \int_0^{\infty} \frac{x \Delta\varphi(x) dx}{x^2 - \omega^2}, \quad (36)$$

where  $R = \tilde{r}\tilde{r}^*$ , and  $\tilde{r} = |\tilde{r}| \exp(i\Delta\varphi)$  is the amplitude reflection coefficient. On the basis of those relations and the Fresnel formulas (6) and (7), one can determine the optical constants  $n$  and  $\kappa$  of the substance.

According to Pekar's theory, if SD in the medium is substantial, the spectra of reflection and phase variation at reflection are described by the same Fresnel formulas, but the "effective" values of  $n$  and  $\kappa$ , which are determined from relations (26) and (26), should be substituted into them. In Fig. 11, *a*, the spectral dependences  $n_{\text{eff}}(\omega)$  and  $\kappa_{\text{eff}}(\omega)$  in the range of  $A_{n=1}$ -exciton in a CdS crystal are depicted (curves 1 and 2, respectively). They were calculated for  $\Gamma = 1 \text{ cm}^{-1} < \Gamma_{cr}$ . A pair of dependences, conjugated to them by relations (21) and (22), were also calculated (curves 3 and 4, respectively). One can see that the agreement between dependences 1 and 3, as well as between 2 and 4, is excellent; hence, *KKR's (21) and (22) hold true, if being applied to the "effective" quantities  $n_{\text{eff}}(\omega)$  and  $\kappa_{\text{eff}}(\omega)$* . Relations (23) and (24) are also obeyed if, by the formal analogy with the single-wave theory, one writes down that  $\varepsilon'_{\text{eff}} = n_{\text{eff}}^2 - \kappa_{\text{eff}}^2$  and  $\varepsilon''_{\text{eff}} = 2n_{\text{eff}}\kappa_{\text{eff}}$ , in spite of the fact that the parameter  $\varepsilon''_{\text{eff}}$  does not now describe energy losses in the crystal. Afterwards, using Pekar's theory and the "effective" quantities  $n_{\text{eff}}$  and  $\kappa_{\text{eff}}$ , the spectra of reflection  $R^P(\omega)$  and reflected wave phase  $\Delta\varphi^P(\omega)$  were calculated (Pekar curves 1 and 2,

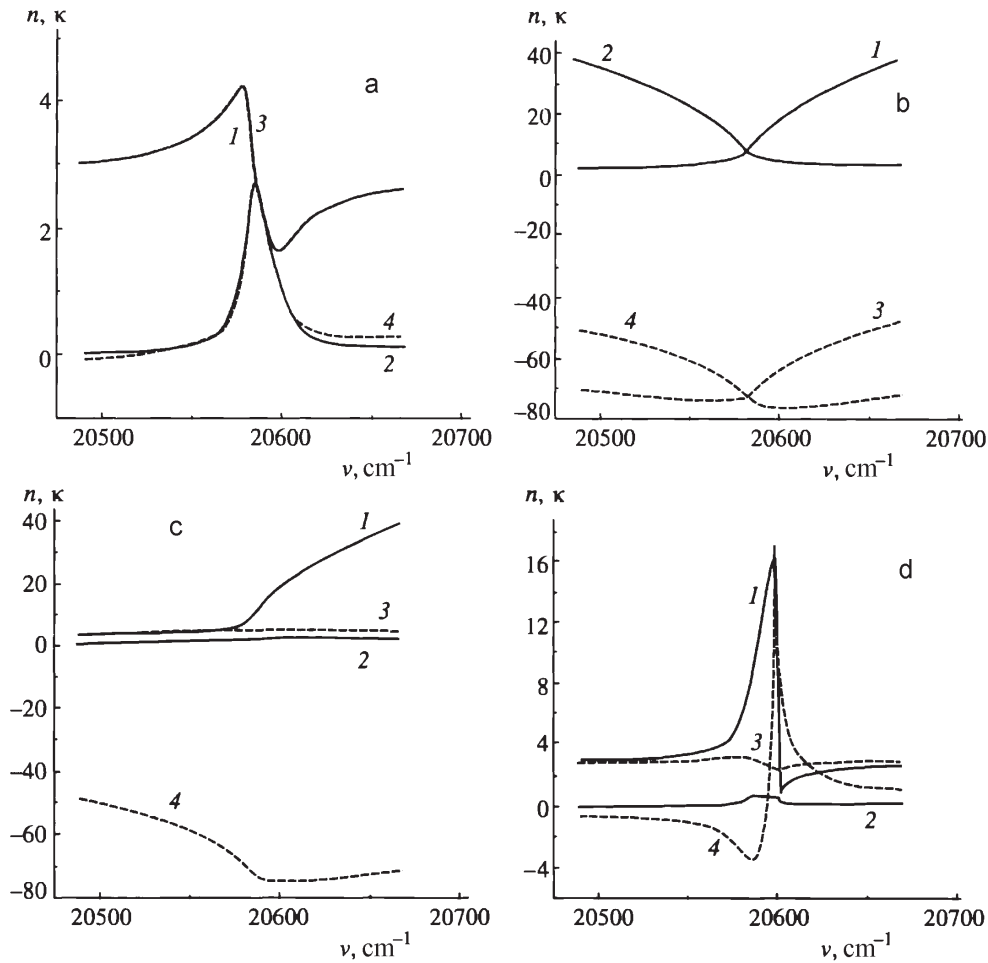


Fig. 10. Pekar's dependences  $n(\omega)$  (1) and  $\kappa(\omega)$  (2) and the corresponding conjugated dependences calculated on their basis by relations (21) and (22) (curves 3 and 4, respectively) for the "plus-minus"-(a) and "minus-plus"-(b) waves at  $\Gamma > \Gamma_{cr}$  and, at  $\Gamma < \Gamma_{cr}$ , for the "+"-(c) and "plus-minus"-waves with matching the solutions at  $\omega_L$  (d) [47]

respectively, in Fig. 11, b). KKR's (35) and (36) were applied to those spectra to calculate the Kramers dependences  $R^K(\omega)$  and  $\Delta\varphi^K(\omega)$  (Kramers curves 4 and 3, respectively). A good agreement between the two curves depicted in Fig. 11 testifies that KKR's (35) and (36) are fulfilled at length, if being applied to the reflection spectra  $R(\omega)$  and  $\Delta\varphi(\omega)$  calculated with the use of  $n_{eff}$  and  $\kappa_{eff}$ .

But, in the case of a DL on the crystal surface, the experimental phase curves  $\Delta\varphi(\omega)$  have either the  $S$ -like or the  $N$ -like shape, depending on the values of parameters  $\Gamma$  and  $d$  (Fig. 6). Let us call the curve, which separates the corresponding ranges of parameters I and II as a threshold curve  $L^{thresh}$ . In works [119, 120], it was shown that if the parameters of reflection spectra correspond to those in curve  $L^{thresh}$ , the minima of the  $R(\omega)$ -curves reach zero.

In works [112–116], the issue of applicability of KKR's (35) and (36) to treat the reflection spectra has been analyzed in detail. It was demonstrated that, at small values of  $\Gamma$ , the following supplementary dispersion relations are valid:

$$\Delta\varphi(\omega) = \frac{\omega}{\pi} \int_0^{\infty} \frac{\ln[R_0/R(x)]}{x^2 - \omega^2} dx + 2 \arctg \frac{\Gamma^{thresh} - \Gamma}{\omega^{thresh} - \omega} + a, \quad (37)$$

$$\ln \frac{R(\omega)}{R_0} = \frac{4}{\pi} \int_0^{\infty} \frac{x[\Delta\varphi(x) - a]}{x^2 - \omega^2} dx + 2 \ln \left[ 1 + \left( \frac{\Gamma^{thresh} - \Gamma}{\omega^{thresh} - \omega} \right)^2 \right]. \quad (38)$$

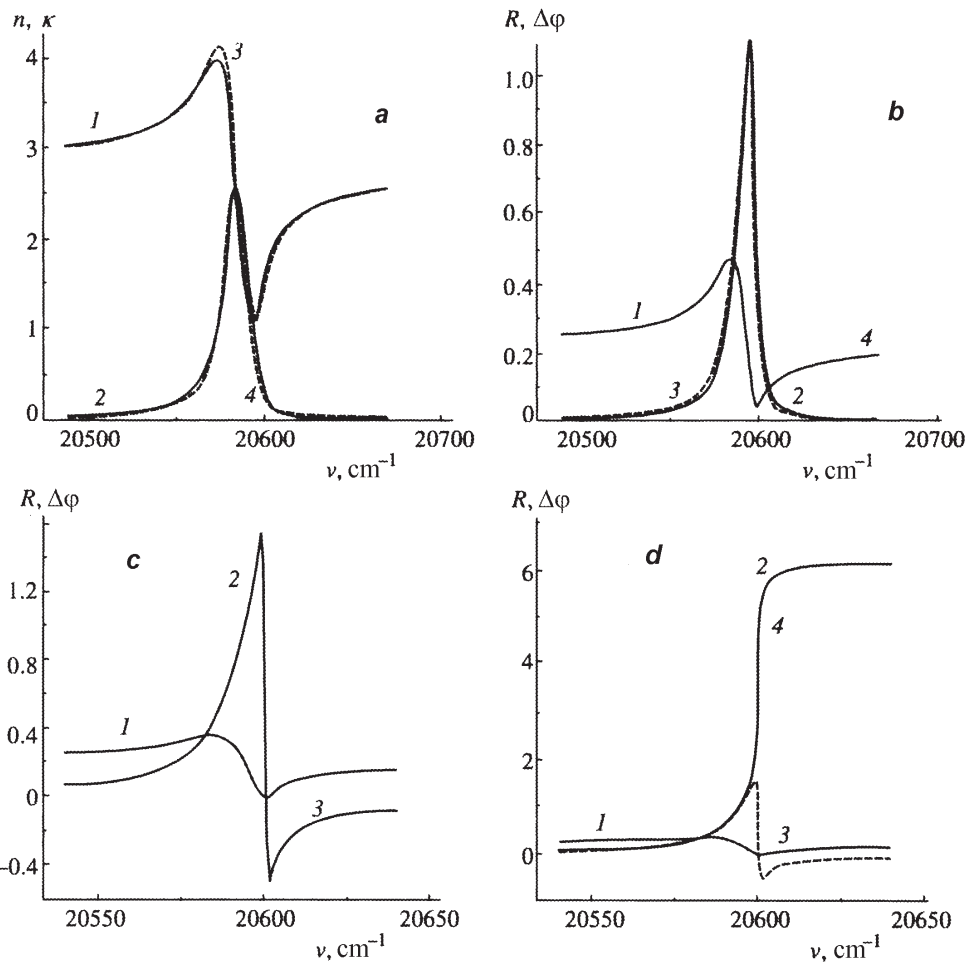


Fig. 11. *a* – Pekar’s dependences  $n_{\text{eff}}(\omega)$  (1) and  $\kappa_{\text{eff}}(\omega)$  (2) and the conjugated dependences calculated by relations (21) and (22) (3 and 4). *b* – Pekar’s spectra of reflection  $R^{\text{P}}(\omega)$  (1) and phase variation at reflection  $\theta^{\text{P}}(\omega)$  (2) and the conjugated dependences calculated by relations (35) and (36) (3 and 4). *c* and *d* –  $R^{\text{P}}(\omega)$  (1) and  $\theta^{\text{P}}(\omega)$  (2) calculated in the framework of Pekar’s theory with a “dead” layer on the crystal surface. Kramers phase spectra  $\theta^{\text{K}}(\omega)$  calculated on the basis of  $R^{\text{P}}(\omega)$  by relation (35) (3) and supplementary relation (37) (4) ( $\Gamma > \Gamma^{\text{thresh}}$  (c) and  $\Gamma < \Gamma^{\text{thresh}}$  (d)) [47]

Here,  $R_0$  is the value of the reflection coefficient far from the resonance;  $\Gamma^{\text{thresh}}$  is the threshold value of the damping constant: the phase curve is *S*-like for  $\Gamma < \Gamma^{\text{thresh}}$  and *N*-like for  $\Gamma > \Gamma^{\text{thresh}}$ ;  $\omega^{\text{thresh}}$  is the frequency, at which the first additional term in formula (37) is equal to  $\pm\pi$ ; and  $a = 0$  at  $\omega < \omega^{\text{thresh}}$  and  $2\pi$  at  $\omega > \omega^{\text{thresh}}$ .

The additional terms in KKR’s appear owing to a singular zero point in the  $R(\omega)$  spectrum. If  $\Gamma < \Gamma^{\text{thresh}}$ , this point is located in the upper half-plane of the complex variable  $\tilde{\omega} = \omega' + i\omega''$ , and, while integrating along the contour  $C$ , it has to be gone around, which gives rise to the appearance of an additional term in

formula (35) and the necessity to add  $2\pi$  at frequencies  $\omega > \omega^{\text{thresh}}$ . If  $\Gamma = \Gamma^{\text{thresh}}$ , the zero point is located on the real axis at the frequency  $\omega^{\text{thresh}}$ , and, if  $\Gamma > \Gamma^{\text{thresh}}$ , it transits into the lower half-plane, so that the additional terms must be rejected. Hence, the curve  $L^{\text{thresh}}$  simultaneously demonstrates that the application of usual KKR’s (35) and (36) is eligible in region II, and the application of KKR’s (37) and (38) is eligible in region I.

In work [47], the intensity and phase reflection spectra in the range of  $A_{n=1}$ -exciton in a CdS crystal were calculated taking the DL into account; the results of calculations are depicted in Figs. 11, c

and *d*. The DL thickness was assumed to be 7 nm. First, in the framework of Pekar's theory and taking the DL into account, the spectra  $R^P(\omega)$  and  $\Delta\varphi^P(\omega)$  were calculated. Then, the obtained reflection spectrum  $R^P(\omega)$  was used to calculate the corresponding Kramers phase curve  $\Delta\varphi^K(\omega)$  – by either relation (35) or (37), – which was compared afterwards with the Pekar phase curve  $\Delta\varphi^P(\omega)$ .

The results of comparison made for two values of  $\Gamma$ , larger and smaller than the threshold value  $\Gamma^{\text{thresh}} = 1.21 \text{ cm}^{-1}$ , are presented in Figs. 11,*c* and *d*, respectively. From Fig. 11,*c*, one can see that, in the presence of a DL and at  $\Gamma > \Gamma^{\text{thresh}}$ , the relation between the phase and amplitude reflection curves is described well by the usual KKR (35). But, in this case, the *N*-like dependence has a negative section; therefore, the optical constants  $n$  and  $\kappa$  determined by formulas (6) and (7) are incorrect. Moreover – and this is more important – a section of negative values, which have no physical sense, automatically appears in the curve  $\kappa(\omega)$  as well. Therefore, a more complicated inverse problem, which takes the DL into consideration, must be solved. Figure 11,*d* demonstrates that, if  $\Gamma < \Gamma^{\text{thresh}}$ , the supplementary dispersion relation (37) is fulfilled well, because phase curves 2 and 4, which are *S*-like, practically coincide with each other. But, if relation (35) had been applied, following the conventional technique of the determination of optical constants, to such reflection spectrum, the incorrect phase curve 3 rather than the correct curve 2 would have been obtained no later than at the first stage of calculations, and, as a result, wrong values for  $n$ ,  $\kappa$ ,  $\varepsilon'$ , and  $\varepsilon''$  would also have been calculated.

Analogous calculations, which were executed for a model of classical oscillator with a DL on the surface, demonstrated that the phase curves also have either an *S*- or an *N*-like shape. Therefore, *it is the DL rather than the spatial dispersion effect that is responsible for such a shape of the curves  $\Delta\varphi(\omega)$* , because, if the medium absorbs, the interference effect is the reason of why the dependence  $R(\omega)$  becomes zero. Therefore, *N*-like curves with negative section can be observed both at relatively high temperatures and in media with negligibly small SD.

Recently, it was shown in work [121] that, in the case of the oblique incidence of light onto a plane-parallel CdSe plate and in the presence of an ALW, a drastic phase jump by  $6\pi$  is possible for the reflected wave at  $\omega \approx \omega_L$ .

## 8. Topicality of ALW Researches

At the end of the description of the activity devoted to studying the SD effects in three-dimensional structures, owing to the restriction imposed upon the review's length, we only briefly indicate those works, where the essential influence of ALWs on optical characteristics of crystals has been demonstrated.

In works [17, 122, 123], the properties of excitons with a complicated band structure, owing to which the propagation of two additional waves in the vicinity of a resonance becomes possible, were studied. In particular, in works [122, 123], the optical activity of a special type and the inversion of the crystal optical axis were observed in CdS crystals in the range of its  $B_{n=1}$ -exciton; these phenomena were described in detail in the review by E.L. Ivchenko [11]. The dispersion of the refractive index with a discontinuity at the frequency  $\omega_0$  was measured in the same crystals in work [17].

In works [40, 124], the analysis of experimental researches of dispersion and absorption in CdS crystals was made, and the data concerning the temperature and frequency dependences of the damping constant of excitons in this medium were obtained. The dependence  $\Gamma(\omega)$  was demonstrated to have a step-like character, with every step being associated with a next, higher-located exciton state. A delta-like peak was associated with the effect of "anticrossing" between the dispersion branches of allowed and forbidden  $A_{n=1}$ -excitons, which was paid attention to in work [28]. At the frequency  $\omega_L$ , the value of  $\Gamma$  grows drastically in comparison with that in the  $\Delta_{LT}$  region. This phenomenon was registered for the first time in works [27, 29]. It is caused by umklapp processes – induced by exciton-phonon interaction – between the upper and the lower polariton branches, as well as by possible mutual transformations of the "+"- and "-"-waves at collision with an arbitrary obstacle (e.g., an impurity), similarly to what takes place at the reflection from the crystal surface. The processes of mutual transformations of the "+", "-", and longitudinal waves at spherical inclusions was considered theoretically in work [125].

Very important is the issue concerning the energy propagation in the resonance range of the spectrum in the presence of ALWs. In work [126], the fluxes of energy in a medium with SD were examined making allowance for absorption; it was shown that the interference between normal waves gives rise to the emergence of interference energy flows. In work [127], expressions for the energy density, the density of energy flow, and the

specific thermal emission in crystals with SD in the spectral range of a quadrupole exciton resonance were obtained. It was shown that the total energy flow is not a simple sum of contributions made by every wave separately: the interference-related flows are substantial and have to be taken into consideration.

Since the speed of signal transfer in a dispersion medium is determined by the group velocity of a wave packet, it is of interest to consider the problem in the presence of ALWs. In work [40], the interference method [128, 129] was used to measure the spectral dependence of the group velocity of the “+”-wave in the range of  $A_{n=1}$ -exciton of a CdS crystal at  $T = 4.2$  K. The speed of a wave packet at its maximal deceleration turned out  $1.3 \times 10^4$  times as lower as the speed of light, which is in good agreement with the result of calculations. By its order of magnitude, this value is close to the value obtained in work [35] for a CuCl crystal, which was measured by the time delay of the picosecond pulse transmission.

An entire domain in optics, exciton luminescence, is also unbrokenly connected with the polariton model. The necessity to engage this model in order to give a qualitative explanation to experimental features of resonance emission has been demonstrated in works by Gross and coauthors [130, 131]. The authors found that the states of the upper polariton branch, which were initially excited, due to their interaction with LO phonons, jump onto the lower polariton branch, and, afterwards, relax along it towards the bottleneck region, where they are accumulated before the emission. Thus, in spite of the fact that the exciton-like branch, which corresponds to the “+”-wave, is not excited by light directly (i.e. its excitation energy considerably exceeds  $\omega_0$ ), it plays a large role in the formation of the luminescence spectrum. The kinetics and luminescence of polaritons were considered in detail in work [132]; in the same work, a large review of the literature on this subject was made.

At last, we would like to note that the account of the dispersion of polariton branches is mandatory in nonlinear optics in the cases where high levels of excitation stimulate the strong exciton-exciton interaction, so that the formation of biexcitons and the hyper-Raman light scattering (see the review by Koteles in collective monograph [11]) become feasible.

## 9. Modern Trends in Studying ALWs

As was already pointed out in Introduction, the rapid development of nanophysics in the early 1990s brought

about a substantial reduction of the number of works devoted to studying the SD effects. But recently, the interest to this subject has been renewed, which is associated with the search for a non-local response to electromagnetic excitations just in new systems. Consider a few directions of studying the SD effects developed within recent years.

The theoretical consideration of various ABCs, as well as the elucidation of their validity in comparison with experiment, has been continued [76, 77, 79, 80, 133, 134]. To the same scope of works can be attributed works [121, 135]. In work [135], the method of exact calculation of the properties of exciton polaritons with SD was developed; it is based on the microtheory of boundary conditions and includes continuum states. The results were compared with those obtained in the framework of macrotheory for various ABCs. The best agreement was attained for Pekar’s ABC with a DL on the surface and taking the continuum states into account, whereas the ABCs proposed in works [67, 76] could not be put in agreement at any values of the parameters.

In experiment, the greatest attention is focused on the researches of the properties of GaAs and AlGaAs/GaAs systems: from the elementary cases of a single quantum well and the structures composed of many quantum wells separated by wide barriers to the formation of a superlattice, where the wave functions overlap in the periodic system of quantum wells. The band structure of GaAs is more complicated than that of CdS, because the degeneration of light ( $l$ ) and heavy ( $h$ ) holes at the point  $K = 0$  is not removed. In GaAs, therefore, there are two exciton bands with different effective masses, and, correspondingly, there may exist two additional waves with different asymptotes.

Very interesting results were obtained in works [136, 137], while studying very thin (500, 200, and 50 nm in thickness) GaAs films by the method of femtosecond spectroscopy, the pump-probe technique. A weak oscillatory structure (a “fringe”) of the absorption spectrum was revealed at  $T = 20$  K; this structure is similar to that observed in works [25–29] but is located much higher than the basic exciton state, in the range of interband transitions. Two periods of oscillations could be neatly distinguished in this structure; therefore, the authors explained the structure as the interference between a photon-like and two exciton-like polariton branches, which corresponds to light and heavy excitons, respectively. The periods of oscillations were used to determine the effective exciton masses in the corresponding bands. Oscillations in the spectrum were observed only after an 80-fs

pump pulse had created a significant (from  $10^{14}$  to  $10^{16}$   $\text{cm}^{-3}$ ) concentration of free carriers along the path of a 17-fs probe pulse. Therefore, the emergence of the “fringe” structure in the absorption spectrum was explained by the authors as that associated with the effective damping of exciton-like polarization owing to the exciton scattering by free carriers. In other words, the pump pulse, being scattered by phonons, fills the states of exciton-like branches which are not excited by photons directly (the process is similar to what happens in luminescence phenomena). This enables them to interfere with a photon-like polariton branch at the probe pulse transmission, whereas, if there is no pumping, the states are not filled and the interference structure is absent.

In works [138, 139], the precision measurements of the intensity and the phase of light transmitted through a high-quality GaAs layer  $0.25 \mu\text{m}$  in thickness, which was sandwiched between AlGaAs layers, were fulfilled. The specimen was imbedded into superfluid helium, and the laser with a pulse duration of 100 fs was used. The authors also developed a microscopic theory which is based on the straightforward solution of the Schrödinger equation for an exciton in specimens, the thickness of which ranges from ten to one – or even less – Bohr radii of an exciton. Theoretical calculations took into account the spatial dispersion, the quantization of the motion of the exciton center of mass, confinements imposed on carriers’ motion, and the characteristic features of the band structure. Agreement between the experimental and calculated curves proved to be very good.

At the same time, the macroscopic theory cannot explain the important features of the transmission spectrum, because the effects of exciton center-of-mass quantization and SD are approximately identical by amplitude. Among various macroscopic models, Pekar’s ABC is always in much better agreement with the complete theory and experiment than the boundary conditions proposed in works [67, 76]. The combination of Pekar’s ABC with a “dead” layer allows one to obtain full agreement with the microtheory. Nevertheless, the thickness of this layer is an extra parameter of the theory and should be determined for every frequency: for exciton states, which are located higher, it becomes reduced. Therefore, a conclusion was drawn that a simultaneous description of the measured amplitude and phase of the transmitted electric field could be obtained only in the framework of the complete model.

Very interesting are the researches of the SD effects in photon crystals, where a spatial periodicity is created by alternating materials with very different dielectric

permittivities. In work [140], theoretical calculations of the optical properties of a multilayered dispersion medium, in which quantum wells were arranged at a distance of  $\lambda/2$  from one another (the condition of Bragg reflection), were fulfilled in the framework of the semiclassical consideration and making allowance for SD. It turned out that the non-local optical response of the system depends very much on the number of quantum wells. The parameters of calculations corresponded to those of the AlGaAs/GaAs system. Polariton dispersion curves were calculated. A large review of the literature was made.

At last, it should be emphasized that the polariton model is used to analyze the luminescence spectra in semiconductor microresonators (see, e.g., work [141] and references therein). The energy relaxation of polaritons in GaAs-based structures differs strongly from the relaxation of bulk polaritons and depends substantially on the conditions of optical excitation and the temperature.

Nowadays, a tendency to look for the SD effects in the long-wave (tera- and gigahertz) frequency range was outlined. For instance, in work [142], the optical properties of layered superconductors in the vicinity of the Josephson plasma resonance were studied. Propagation and reflection of light were theoretically considered for its normal and oblique incidence onto the surfaces of these strongly anisotropic crystals with SD; the surfaces were considered to be oriented normally or in parallel to the layers. The case with a negative effective mass,  $M < 0$ , attracts a special attention (Fig. 1, *b*). At the frequency which corresponds to the return point of real  $n^2$ -values and where the  $n_+$ - and  $n_-$ -branches transform into each other, the group velocity of the wave packet becomes zero. In an ideal case where the damping is absent, i.e. at  $\Gamma = 0$ , light has to stop. Under those conditions, the Fresnel approximation was shown to become incorrect near the return point. (The authors do not seemingly know the works concerning the invalidity of the Fresnel formulas in the whole resonance range rather than at a single point only, which were discussed in Section 4.) An assumption was made that, in media with SD, conditions could be provided for the light pulse to stop, which would open ample opportunities for the implementation of the method in quantum information science.

These researches were continued in work [143], phonon polaritons in ionic crystals being the matter of interest. The influence of SD of phonon modes on the reflection spectrum has been studied. It has been demonstrated that, provided the values of the

damping constant are very small, the reflection spectra for positive and negative effective masses are strongly different in the region of the  $R(\omega)$ -curve minimum.

In work [144], an artificial medium (metamaterial) was considered. The medium was formed by a grid of thin parallel wires. SD of this system was shown to be very strong at any frequency, including very long waves. A dramatic difference in the predicted behavior of this medium with respect to the propagation of electromagnetic waves in it was demonstrated for the local and non-local models of susceptibility. Therefore, to describe such media, one must use a theory that takes SD into consideration.

## 10. Conclusions

The experimental data, which were discussed in this review, convincingly evidence for the existence of additional light waves predicted by S.I. Pekar in 1957. These waves may manifest themselves if one studies light that is reflected by, scattered in, or transmitted through a crystal. They were managed to be separated in space from the ordinary waves and directly observed after light transmission through a wedge-shaped crystal.

At present time, generalized crystal optics, which takes SD into account, is an integral part of solid state physics. It does not only explain the features of observed spectral characteristics, but also produces results that agree with them quantitatively. The interaction between light and crystals at low temperatures has to be described by the relations of this theory, because classical single-wave crystal optics proves to be incorrect: the KKR's and the Fresnel formulas are not obeyed; measurements of the refractive index, which are based on the phase variation of a light wave transmitted through a crystal, give such "effective" values in the actual range of exciton spectrum that depend on the specimen thickness.

The transition to single-wave crystal optics occurs when the constant of exciton damping exceeds some critical value, which corresponds to a certain critical temperature. The critical values of  $\Gamma$  depend on parameters that characterize the exciton band and differ very strongly for different substances. Moreover, the critical temperature may be different for the same substance, because it depends on the degree of crystal perfection, impurities, and distortion of a specific specimen. Therefore, the determination of the critical temperature of the specimen and, hence, the establishment of whether the relations of the single-wave theory are applicable in every specific case demand that an additional analysis should be done.

Special care should be exercised while determining the optical constants of a substance from its reflection spectra – the method, which is widely used in optics owing to its relative simplicity and the availability of the required facilities. First, one should bear in mind that, in the case where SD is essential, the reflection spectrum is formed by the effective refractive index, which is an involved combination of the parameters of both waves that are excited in the crystal. Therefore, if the KKR's of the single-wave theory were applied in this case to determine  $n$  and  $\kappa$ , the basis for a wrong result might be laid already at the initial stage of calculations. Second, additional difficulties arise due to the presence of an intrinsic "dead" layer on the crystal surface. At last, the properties of a crystal in the near-surface region can differ from those in the bulk, so that the formation of a non-intrinsic surface layer also becomes possible, which would introduce additional complications into the problem.

The researches of the SD effects and Pekar's ALWs become more intense as modern technologies are developed aiming at growing high-quality layered structures with quantum wells and superlattices. The search for a non-local response to electromagnetic excitation is carried on in wider and wider ranges of wavelengths and in novel media, including superconductors and metal-wire gratings. A possibility of creating the media with SD to delay light pulses is examined. In the media with a negative effective mass, the deceleration effect for the wave-packet group velocity should be maximal.

Taking the aforesaid into account, one can expect that, in the nearest future, the number of works dealing with the study of the SD effects in novel media should increase, especially in connection with the search for their implementations in new devices.

1. S.I. Pekar, Zh. Èksp. Teor. Fiz. **33**, 1022 (1957).
2. S.I. Pekar, *Phenomenon of Additional Light Wave (Pekar Wave) Propagation in Crystals*, Discovery Diploma N 323, applied on 27.09.84, published on 30.08.87 (State Committee on Inventions and Discoveries of the USSR) (in Russian); Otkryt. Izobret. N 32, 3 (1987).
3. M.S. Brodin and A.F. Prikhot'ko, Opt. Spektrosk. **2**, 448 (1957).
4. M.S. Brodin and M.S. Soskin, Izv. Akad. Nauk SSSR, Ser. Fiz. **22**, 1316 (1958).
5. M.S. Brodin, A.F. Prikhot'ko, and M.S. Soskin, Opt. Spektrosk. **6**, 28 (1959).
6. M.S. Brodin and M.I. Strashnikova, Fiz. Tverd. Tela **4**, 2454 (1962).

7. M.S. Brodin and S.I. Pekar, Zh. Èksp. Teor. Fiz. **38**, 74 (1960); **38**, 1910 (1960).
8. I.S. Gorban and V.B. Timofeev, Dokl. Akad. Nauk SSSR **140**, 791 (1961).
9. J.J. Hopfield and D.G. Thomas, Phys. Rev. **132**, 563 (1963).
10. V.M. Agranovich and V.L. Ginzburg, *Spatial Dispersion in Crystal Optics and the Theory of Excitons* (Wiley, London, 1966); V.M. Agranovich and V.L. Ginzburg, *Crystal Optics with Spatial Dispersion and Excitons*, 2nd ed. (Springer, Berlin, 1984).
11. J.L. Birman, in *Excitons*, edited by E.I. Rashba and M.D. Sturge (North-Holland, Amsterdam, 1987), Ch. 2; E.S. Koteles, *ibid.*, Ch. 3; E.L. Ivchenko, *ibid.*, Ch. 4.
12. S.I. Pekar, *Crystal Optics and Additional Light Waves* (Benjamin/Cummings, Menlo Park, Calif., 1983).
13. R.S. Knox, *Theory of Excitons* (Academic Press, New York, 1963).
14. A.S. Davydov, *Theory of Solid State* (Nauka, Moscow, 1976) (in Russian).
15. *Cryocrystals*, edited by B.I. Verkin and A.F. Prikhot'ko (Naukova Dumka, Kyiv, 1983) (in Russian).
16. M.V. Lebedev, M.I. Strashnikova, V.B. Timofeev, and V.V. Chernyi, Pis'ma Zh. Èksp. Teor. Fiz. **39**, 366 (1984).
17. M.V. Lebedev, M.I. Strashnikova, V.B. Timofeev, and V.V. Chernyi, Fiz. Tverd. Tela **29**, 1948 (1987).
18. M.I. Strashnikova, Ukr. Fiz. Zh. **37**, 505 (1992).
19. L.D. Landau and E.M. Lifshits, *Electrodynamics of Continuous Media* (Pergamon, New York, 1984).
20. V.L. Ginzburg, Zh. Èksp. Teor. Fiz. **34**, 1593 (1958).
21. E.F. Gross and A.A. Kaplyanskii, Dokl. Akad. Nauk SSSR **132**, N 1, 98 (1960).
22. I.S. Gorban and V.B. Timofeev, Fiz. Tverd. Tela **2**, 2077 (1960).
23. J.J. Hopfield, Phys. Rev. **112**, 1575 (1958).
24. K.B. Tolpygo, Zh. Èksp. Teor. Fiz. **20**, 497 (1950).
25. V.A. Kiselev, B.S. Razbirin, and I.N. Uraltsev, Pis'ma Zh. Èksp. Teor. Fiz. **18**, 504 (1973).
26. V.A. Kiselev, B.S. Razbirin, and I.N. Uraltsev, in *Proceedings of the 12-th International Conference on Physics of Semiconductors, Stuttgart, July 1974* (Teubner, Stuttgart, 1974), p. 1036.
27. V.A. Kiselev, B.S. Razbirin, and I.N. Uraltsev, Phys. Status Solidi B **72**, 161 (1975).
28. V.A. Kiselev, B.S. Razbirin, I.N. Uraltsev, and V.P. Kochereshko, Fiz. Tverd. Tela **17**, 640 (1975).
29. I.V. Makarenko, I.N. Uraltsev, and V.A. Kiselev, Phys. Status Solidi B **98**, 773 (1980).
30. W. Brenig, R. Zeyher, and J.L. Birman, Phys. Rev. B **6**, 4612 (1972).
31. R.G. Ulbrich and C. Weisbuch, Phys. Rev. Lett. **38**, 865 (1977).
32. G. Winterling and E.S. Koteles, Solid State Commun. **23**, 95 (1977).
33. T. Goto and Y. Nishina, Solid State Commun. **31**, 751 (1979).
34. E.S. Koteles and G. Winterling, Phys. Rev. B **20**, 628 (1979).
35. Y. Masumoto, Y. Unuma, Y. Tanaka, and S. Shionoya, J. Phys. Soc. Jpn. **47**, 1844 (1979).
36. S.I. Pekar, Zh. Èksp. Teor. Fiz. **34**, 1176 (1958).
37. I. Broser, R. Broser, E. Beckmann, and E. Birkicht, Solid State Commun. **39**, 1209 (1981).
38. A.A. Demidenko, S.I. Pekar, B.I. Tsekvava, Fiz. Tverd. Tela **27**, 743 (1985).
39. A.A. Demidenko, M.I. Lebedev, S.I. Pekar, M.I. Strashnikova, V.B. Timofeev, and B.I. Tsekvava, Zh. Èksp. Teor. Fiz. **89**, 330 (1985).
40. V.Ya. Reznichenko, M.I. Strashnikova, and V.V. Chernyi, Pis'ma Zh. Èksp. Teor. Fiz. **49**, 574 (1989).
41. M.I. Strashnikova and A.T. Rudchik, Fiz. Tverd. Tela **14**, 984 (1972).
42. M.S. Brodin, N.A. Davydova, and M.I. Strashnikova, Pis'ma Zh. Èksp. Teor. Fiz. **19**, 567 (1974).
43. M.I. Strashnikova, Fiz. Tverd. Tela **17**, 729 (1975).
44. T.S. Moss, G.J. Burrell, and B. Ellis, *Semiconductor Opto-Electronics* (Butterworths, London, 1973).
45. H.M. Nussenzweig, *Causality and Dispersion Relations* (Academic Press, New York, 1972).
46. V.V. Sobolev and V.V. Nemoshkalenko, *Methods of Computational Physics in Solid State Theory* (Naukova Dumka, Kyiv, 1988) (in Russian).
47. M.I. Strashnikova and E.V. Mozdor, Zh. Èksp. Teor. Fiz. **114**, 1393 (1998).
48. S.I. Pekar and M.I. Strashnikova, Zh. Èksp. Teor. Fiz. **68**, 2047 (1975).
49. L.E. Solov'ev and A.B. Babinskii, Pis'ma Zh. Èksp. Teor. Fiz. **23**, 291 (1976).
50. A.V. Komarov, S.M. Ryabchenko, and M.I. Strashnikova, Zh. Èksp. Teor. Fiz. **74**, 251 (1978).
51. A.B. Pevtsov, S.A. Permogorov, Sh.R. Saifulaev, and A.V. Selkin, Fiz. Tverd. Tela **22**, 2400 (1980).
52. V.A. Kiselev, I.N. Uraltsev, and I.V. Makarenko, Solid State Commun. **53**, 591 (1985).
53. V.Ya. Reznichenko, M.I. Strashnikova, and V.V. Chernyi, Phys. Status Solidi B **152**, 675 (1989).
54. M.I. Strashnikova and E.V. Mozdor, Zh. Èksp. Teor. Fiz. **129**, 474 (2003).
55. A.A. Delyukov and G.V. Klimusheva, Fiz. Tverd. Tela **16**, 3255 (1974).
56. A.S. Davydov and E.N. Myasnikov, Phys. Status Solidi B **63**, 325 (1974).
57. M.I. Strashnikova and E.V. Bessonov, Zh. Èksp. Teor. Fiz. **74**, 2206 (1978).
58. J. Voigt, Phys. Status Solidi B **64**, 549 (1974).
59. B. Dietrich and J. Voigt, Phys. Status Solidi B **93**, 669 (1979).
60. N.N. Akhmediev, Zh. Èksp. Teor. Fiz. **79**, 1534 (1980).

61. N.N. Akhmediev, G.P. Golubev, V.S. Dneprovskii, and A.E. Zhukov, *Fiz. Tverd. Tela* **25**, 2225 (1983).
62. A.B. Novikov, L.E. Solov'ev, and V.G. Talalaev, *Fiz. Tverd. Tela* **28**, 1931 (1986).
63. S.R. Grigoryev, S.B. Moskovskii, A.B. Novikov, and L.E. Solov'ev, *Vestn. Leningr Gos. Univ., Ser. 4, N 3* (1987).
64. M.S. Brodin, N.A. Davydova, and M.I. Strashnikova, *Phys. Status Solidi B* **70**, 365 (1975).
65. M.V. Lebedev, V.G. Lysenko, and V.B. Timofeev, *Zh. Èksp. Teor. Fiz.* **86**, 2193 (1984).
66. M.I. Strashnikova and V.V. Chernyi, *Fiz. Tverd. Tela* **33**, 1134 (1991).
67. C.S. Ting, M.J. Frankel, and I.L. Birman, *Solid State Commun.* **17**, 1285 (1975).
68. V.I. Sugakov, *Fiz. Tverd. Tela* **5**, 2207 (1963); **5**, 2682 (1963).
69. V.I. Sugakov, *Fiz. Tverd. Tela* **6**, 1361 (1964).
70. V.I. Sugakov, *Fiz. Tverd. Tela* **14**, 1977 (1972).
71. C.W. Deutsche and C.A. Mead, *Phys. Rev.* **138A**, 63 (1965).
72. S.I. Pekar, *Zh. Èksp. Teor. Fiz.* **74**, 1458 (1978).
73. A.A. Maradudin and D.L. Mills, *Phys. Rev. B* **7**, 2787 (1973).
74. G.S. Agarval, D.N. Pattanayak, and E. Wolf, *Phys. Rev. B* **10**, 1447 (1974).
75. A.S. Davydov and A.A. Eremko, *Ukr. Fiz. Zh.* **18**, 1863 (1973).
76. K. Henneberger, *Phys. Rev. Lett.* **80**, 2889 (1998).
77. D.F. Nelson and B. Chen, *Phys. Rev. Lett.* **83**, 1263 (1999).
78. R. Zeyher, *Phys. Rev. Lett.* **83**, 1264 (1999).
79. K. Henneberger, *Phys. Rev. Lett.* **83**, 1265 (1999).
80. E.F. Venger and V.N. Piskovoi, *Phys. Rev. B* **70**, 115107 (2004).
81. A.S. Davydov and E.N. Myasnikov, in *Excitons in Molecular Crystals* (Naukova Dumka, Kyiv, 1973), p. 42 (in Russian).
82. V.A. Kiselev, *Fiz. Tverd. Tela* **20**, 2173(1978); **21**, 1069 (1979).
83. F. Evangelisti, A. Frova, and F. Patella, *Phys. Rev. B* **10**, 4253 (1974).
84. T.M. Mashlyatina, D.S. Nedzvetskii, and L.E. Solov'ev, *Fiz. Tverd. Tela* **21**, 2040 (1979).
85. W. Stossel and H.Y. Wagner, *Phys. Status Solidi B* **89**, 403 (1978).
86. Y. Broser, M. Rosenzweig, R. Broser, M. Richard, E.A. Birckicht, *Phys. Status Solidi B* **90**, 77 (1978).
87. S.V. Marisova, *Opt. Spektrosk.* **22**, 566 (1967).
88. M.S. Brodin, S.V. Marisova, and S.A. Shturkhetskaya, *Ukr. Fiz. Zh.* **13**, 353 (1968).
89. M.S. Brodin, M.A. Dudinskii, S.V. Marisova, and V.I. Sugakov, in *Modern Problems in Optics and Nuclear Physics* (Naukova Dumka, Kyiv, 1974), p.38 (in Russian).
90. A.S. Batyrev, V.A. Kiselev, B.V. Novikov, and A.E. Cherednichenko, *Zh. Èksp. Teor. Fiz.* **39**, 436 (1984).
91. N.A. Davydova, E.N. Myasnikov, and M.I. Strashnikova, *Fiz. Tverd. Tela* **15**, 3332 (1973); **16**, 1173 (1974).
92. E. Skaistis and V.I. Sugakov, *Litov. Fiz. Sborn. N 2*, 297 (1974) (in Russian).
93. M.S. Brodin, P.S. Kosobutskii, and S.G. Shevel, *Fiz. Tverd. Tela* **21**, 2510 (1979).
94. T. Lagois and K. Hummer, *Phys. Status Solidi B* **72**, 393 (1975).
95. S.A. Permogorov, V.V. Travnikov, and A.V. Selkin, *Fiz. Tverd. Tela* **14**, 3642 (1972).
96. V.A. Kiselev, B.V. Novikov, A.E. Cherednichenko, and E.A. Ubushiev, *Phys. Status Solidi B* **133**, 573 (1986).
97. M.S. Brodin, A.V. Kritskii, E.N. Myasnikov, M.I. Strashnikova, and L.A. Shlyakhova, *Ukr. Fiz. Zh.* **18**, 828 (1973).
98. G.V. Benemanskaya, B.V. Novikov, and A.E. Cherednichenko, *Fiz. Tverd. Tela* **19**, 1389 (1977).
99. A.S. Batyrev, B.V. Novikov, and A.E. Cherednichenko, *Fiz. Tverd. Tela* **23**, 2989 (1981).
100. N.A. Davydova and I.Yu. Shablii, *Fiz. Tverd. Tela* **24**, 1547 (1982).
101. V.A. Tyagai, V.N. Bondarenko, and O.V. Snitko, *Fiz. Tekh. Poluprovodn.* **5**, 1038 (1971).
102. F. Evangelisti, J.U. Fischbach, and A. Frova, *Phys. Rev. B* **9**, 1516 (1974).
103. B.V. Novikov, A.B. Pavlov, and V.G. Talalaev, *Fiz. Tverd. Tela* **23**, 1014 (1981).
104. S.B. Anokhin, B.V. Novikov, and V.G. Talalaev, *Fiz. Tverd. Tela* **22**, 1787 (1980).
105. V.A. Kiselev, B.V. Novikov, and A.E. Cherednichenko, *Exciton Spectroscopy of Near-Surface Area of Semiconductors* (Leningrad Univ. Publ. House, Leningrad, 1987) (in Russian).
106. H.A. Kramers, *Atti Congr. Int. Fis. Como* **2**, 545 (1927).
107. R. de L. Kronig, *J. Opt. Soc. Am. Rev. Sci. Instrum.* **12**, 547 (1926).
108. M.A. Leontovich, *Zh. Èksp. Teor. Fiz.* **40**, 907 (1961).
109. A.S. Davydov, *Zh. Èksp. Teor. Fiz.* **43**, 1832 (1962).
110. C.A. Mead, *Radiat. Res.* **20**, 101 (1963).
111. V.L. Ginzburg and N.N. Meiman, *Zh. Èksp. Teor. Fiz.* **46**, 243 (1964).
112. S.B. Moskovskii and L.E. Solov'ev, *Zh. Èksp. Teor. Fiz.* **86**, 1419 (1984).
113. S.B. Moskovskii, A.B. Novikov, and L.E. Solov'ev, *Fiz. Tverd. Tela* **30**, 1431 (1988).
114. T. Musienko, V. Rudakov, and L. Solov'ev, *J. Phys.: Condens. Matter* **1**, 6745 (1989).
115. S.B. Moskovskii, A.B. Novikov, O.S. Omegov et al., *Fiz. Tverd. Tela* **33**, 657 (1991).
116. S.B. Moskovskii, A.B. Novikov, and L.E. Solov'ev, *Zh. Èksp. Teor. Fiz.* **105**, 994 (1994).
117. V.N. Piskovoi, private communication.
118. V.I. Gavrilenko, A.M. Grekhov, D.V. Korbutyak, and V.G. Litovchenko, *Optical Properties of Semiconductors. A Handbook* (Naukova Dumka, Kyiv, 1987) (in Russian).
119. A.B. Pevtsov and A.V. Selkin, *Zh. Èksp. Teor. Fiz.* **83**, 516 (1982).

120. A.B. Pevtsov, S.A. Permogorov, and A.V. Selkin, Pis'ma Zh. Èksp. Teor. Fiz. **39**, 261 (1984).
121. Yu.V. Moskalev, S.B. Moskovskii, and L.E. Solov'ev, Opt. Spektrosk. **94**, 238 (2003).
122. E.L. Ivchenko, S.A. Permogorov, and A.V. Selkin, Pis'ma Zh. Èksp. Teor. Fiz. **27**, 27 (1978); **28**, 649 (1978).
123. E.L. Ivchenko and A.V. Selkin, Zh. Èksp. Teor. Fiz. **76**, 1837 (1979).
124. V.Ya. Reznichenko, M.I. Strashnikova, and V.V. Cherny, Phys. Status Solidi B **167**, 311 (1991).
125. Yu.V. Kryuchenko and V.J. Sugakov, Phys. Status Solidi B **111**, 177 (1982).
126. A.V. Selkin, Phys. Status Solidi B **83**, 47 (1977).
127. A.A. Demidenko and V.I. Pipa, Ukr. Fiz. Zh. **38**, 1031 (1993).
128. G.K. Vlasov, A.V. Kritskii, and Yu.A. Kupchenko, Zh. Èksp. Teor. Fiz. **72**, 2064 (1977).
129. M.I. Strashnikova, Opt. Spektrosk. **93**, 142 (2002).
130. E.F. Gross, S.A. Permogorov, V.V. Travnikov, and A.V. Selkin, Fiz. Tverd. Tela **13**, 699 (1971).
131. E. Gross, S. Permogorov, V. Travnikov, and A. Selkin, Solid State Commun. **10**, 1071 (1972).
132. V.V. Travnikov and V.V. Krivolapchuk, Zh. Èksp. Teor. Fiz. **85**, 2087 (1983).
133. B. Chen and D.F. Nelson, Phys. Rev. B **48**, 15372 (1993).
134. V.N. Piskovoi, E.F. Venger, and I.M. Strelniker, Phys. Rev. B **66**, 115402 (2002).
135. E.A. Muljarov and R. Zimmermann, Phys. Rev. B **66**, 235319 (2002).
136. A. Leitenstorfer, G. Goger, M. Betz, M. Bichler, W. Wegscheider, and G. Abstreiter, in *Proceedings of the 12th International Conference on Ultrafast Phenomena, Charleston, SC, USA, 9–13 July, 2000*, p. 357.
137. G. Goger, M. Betz, A. Leitenstorfer, M. Bichler, W. Wegscheider, and G. Abstreiter, Phys. Rev. Lett. **84**, 5812 (2000).
138. J. Tignon, T. Hasche, D.S. Chemla, H.C. Schneider, F. Jahnke, and S.V. Koch, Phys. Rev. Lett. **84**, 3382 (2000).
139. H.C. Schneider, F. Jahnke, S.V. Koch, J. Tignon, T. Hasche, and D.S. Chemla, Phys. Rev. B **63**, 045202 (2001).
140. L. Pilozzi, A. D'Andrea, and K. Cho, Phys. Rev. B **69**, 205311 (2004).
141. D.N. Krizhanovskii, M.N. Makhonin, A.I. Tartakovskii, and V.D. Kulakovskii, Zh. Èksp. Teor. Fiz. **127**, 141 (2005).
142. Ch. Helm and L.N. Bulaevskii, Phys. Rev. B **66**, 094514 (2002).
143. I. Kaelin, Ch. Helm, and G. Blatter, Phys. Rev. B **68**, 012302 (2003).
144. P.A. Belov, R. Marques, S.I. Maslovski, I.S. Nefedov, M. Silveirinha, C.R. Simovski, and S.A. Tretyakov, Phys. Rev. B **67**, 113103 (2003).

Received 09.02.07.

Translated from Ukrainian by O.I. Voitenko

#### ВПЛИВ ДОДАТКОВИХ СВІТЛОВИХ ХВИЛЬ ПЕКАРА НА ОПТИЧНІ СПЕКТРИ КРИСТАЛІВ (ОГЛЯД)

*М.І. Страшнікова*

#### Резюме

Зроблено огляд експериментальних робіт, котрі підтверджують існування додаткових світлових хвиль (ДСХ) в області екситонних резонансів, які були передбачені С.І. Пекаром у 1957 р. Огляд охоплює роботи з вимірювання спектрів поглинання, відбиття, розсіяння, зміни фази світлової хвилі при відбитті, а також з вимірювання дисперсії показника заломлення. Докладно розглянуто роботи з просторового відокремлення хвиль Пекара в тонких клиноподібних кристалах. Відслідковано перехід до однохвильової класичної кристалооптики, який відбувається після досягнення деякого критичного значення константи затухання екситонів. Наведено критерії застосовності класичних співвідношень Крамерса–Кроніга (СКК) і формул Френеля для визначення оптичних характеристик кристалів. Розглянуто особливості апроксимації спектрів відбиття з різними додатковими граничними умовами, а також вплив обробки поверхні на контури екситонних спектрів відбиття.